Computing Riemann Theta Functions

Bernard Deconinck* Matthias Heil† Alexander Bobenko† Mark van Hoeij‡
Marcus Schmies†

AMS subject classification:
14K25, 30E10, 33F05, 65D20

Keywords:
Riemann Theta Function, Pointwise Approximation, Uniform Approximation

June 7, 2002

Abstract

The Riemann theta function is a complex-valued function of g complex variables. It appears in the construction of many (quasi-) periodic solutions of various equations of mathematical physics. In this paper, algorithms for its computation are given. First, a formula is derived allowing the pointwise approximation of Riemann theta functions, with arbitrary, user-specified precision. This formula is used to construct a uniform approximation formula, again with arbitrary precision.

1 Motivation

An Abelian function is a $2g$-fold periodic, meromorphic function of g complex variables. Thus, Abelian functions are generalizations of elliptic functions to more than one variable. Just as elliptic functions are associated with elliptic surfaces, *i.e.*, Riemann surfaces of genus 1, Abelian functions are associated to Riemann surfaces of higher genus. As in the elliptic case, any Abelian function can be expressed as a ratio of homogeneous polynomials of an auxiliary function, the Riemann theta function [11]. Many differential equations of mathematical physics have solutions that are written in terms of Abelian functions, and thus in terms of Riemann theta functions (see [3, 7] and references therein). Thus, to compute these solutions, one needs to compute either Abelian functions or theta functions. Whittaker and Watson [20, §21.1] state "When it is desired to obtain definite numerical results in problems involving Elliptic functions, the calculations are most simply performed with the aid of certain auxiliary functions known as *Theta-functions*." Whittaker and Watson are referring to Jacobi's theta functions, but the same can be said for Abelian functions,

*Department of Mathematics, Colorado State University, Fort Collins, CO 80523-1874, USA
†Fachbereich Mathematik, Technische Universität Berlin, Strasse des 17.Juni 136, 10623 Berlin, Germany
‡Department of Mathematics, Florida State University, Tallahassee, FL 32306, USA

using the Riemann theta function. This paper addresses the problem of computing values of the Riemann theta function and its derivatives.

2 Definition

The Riemann Theta function is defined by

$$\theta(\boldsymbol{z}|\boldsymbol{\Omega}) = \sum_{\boldsymbol{n}\in\mathbb{Z}^g} e^{2\pi i(\frac{1}{2}\boldsymbol{n}\cdot\boldsymbol{\Omega}\cdot\boldsymbol{n}+\boldsymbol{n}\cdot\boldsymbol{z})}, \tag{1}$$

where $\boldsymbol{z} \in \mathbb{C}^g$, $\boldsymbol{\Omega} \in \mathbb{C}^{g\times g}$, such that $\boldsymbol{\Omega}$ is symmetric ($\boldsymbol{\Omega}^T = \boldsymbol{\Omega}$) and the imaginary part of $\boldsymbol{\Omega}$, $\mathrm{Im}(\boldsymbol{\Omega})$, is strictly positive definite. Such an $\boldsymbol{\Omega}$ is called a Riemann matrix. Also, $\boldsymbol{n}\cdot\boldsymbol{z} = \sum_{i=1}^{g} n_i z_i$, the scalar product of the integer vector $\boldsymbol{n}$ with $\boldsymbol{z}$; and $\boldsymbol{n}\cdot\boldsymbol{\Omega}\cdot\boldsymbol{n} = \sum_{i,j=1}^{g} \Omega_{ij} n_i n_j$. The positive definiteness of $\mathrm{Im}(\boldsymbol{\Omega})$ guarantees the convergence of (1), for all values of $\boldsymbol{z}$. Then the series (1) converges absolutely in both $\boldsymbol{z}$ and $\boldsymbol{\Omega}$, and uniformly on compact sets. Thus, it defines a holomorphic function of both $\boldsymbol{z}$ and $\boldsymbol{\Omega}$. The function defined by (1) is also known as a multidimensional theta function, or as a theta function of several variables. There are as many different conventions for writing the Riemann theta function as there are names for it. These different conventions differ from (1) by at worst a complex scaling transformation on the arguments. An extensive overview of the wealth of properties of $\theta(\boldsymbol{z}|\boldsymbol{\Omega})$ is found in [14, 15, 16].

Remarks

- The Riemann theta function was devised by Riemann as a generalization of Jacobi's theta functions of one variable [12], for solving the Jacobi inversion problem on general compact connected Riemann surfaces [17]. For these purposes Riemann considered only theta functions associated with Riemann surfaces. Riemann theta functions in their full generality, as defined in (1), were considered first by Wirtinger [21], whose convention for the arguments is adopted here.

- Often, so-called Riemann theta functions with characteristics are considered [14]. Such theta functions with characteristics are up to an exponential factor Riemann theta functions (1) evaluated at a shifted argument. Thus the computation of the Riemann theta function (1) also allows the computation of theta functions with arbitrary characteristics.

- In many applications, the Riemann theta function (1) originates from a specific Riemann surface, *i.e.*, the Riemann matrix $\boldsymbol{\Omega}$ is the normalized periodmatrix of the Riemann surface. Obtaining this periodmatrix is a nontrivial problem, which is now also reduced to a black-box program. This issue was addressed in [6].

- Some of the algorithms given in this paper have been used already by some of the authors (For instance, tori with constant mean curvature, and Willmore tori with umbilic lines were constructed in [10] using the results of [2, 4]; multiphase solutions of the Kadomtsev-Petviashvili equation were constructed using Schottky uniformization in [3, 5]) but they were not easily available for use by others. Now, these algorithms are implemented as black-box programs

in Maple and Java. The maple implementation is included in the Maple distribution as of Maple 8. It is also available from `http://www.math.fsu.edu/ hoeij/RiemannTheta/`. The Java implementation is available from `www-sfb288.math.tu-berlin.de/ jem`. These implementations are discussed in the appendices.

3 Rewriting the Riemann theta function

The Fourier series representation (1) is the starting point for the computation of Riemann theta functions. Separating both $\boldsymbol{z}$ and $\boldsymbol{\Omega}$ in their real and imaginary parts, $\boldsymbol{z} = \boldsymbol{x} + i\boldsymbol{y}$, $\boldsymbol{\Omega} = \boldsymbol{X} + i\boldsymbol{Y}$, and using $\boldsymbol{Y} = \boldsymbol{Y}^T$, we obtain

$$\begin{aligned}
\theta(\boldsymbol{z}|\boldsymbol{\Omega}) &= \sum_{\boldsymbol{n}\in\mathbb{Z}^g} e^{2\pi i\left(\frac{1}{2}\boldsymbol{n}\cdot\boldsymbol{\Omega}\cdot\boldsymbol{n}+\boldsymbol{n}\cdot\boldsymbol{z}\right)} \\
&= \sum_{\boldsymbol{n}\in\mathbb{Z}^g} e^{2\pi i\left(\frac{1}{2}\boldsymbol{n}\cdot\boldsymbol{X}\cdot\boldsymbol{n}+\boldsymbol{n}\cdot\boldsymbol{x}+i\left(\frac{1}{2}\boldsymbol{n}\cdot\boldsymbol{Y}\cdot\boldsymbol{n}+\boldsymbol{n}\cdot\boldsymbol{y}\right)\right)} \\
&= \sum_{\boldsymbol{n}\in\mathbb{Z}^g} e^{2\pi i\left(\frac{1}{2}\boldsymbol{n}\cdot\boldsymbol{X}\cdot\boldsymbol{n}+\boldsymbol{n}\cdot\boldsymbol{x}\right)} e^{-2\pi\left(\frac{1}{2}\boldsymbol{n}\cdot\boldsymbol{Y}\cdot\boldsymbol{n}+\boldsymbol{n}\cdot\boldsymbol{y}\right)} \\
&= \sum_{\boldsymbol{n}\in\mathbb{Z}^g} e^{2\pi i\left(\frac{1}{2}\boldsymbol{n}\cdot\boldsymbol{X}\cdot\boldsymbol{n}+\boldsymbol{n}\cdot\boldsymbol{x}\right)} e^{-2\pi\left(\frac{1}{2}(\boldsymbol{n}+\boldsymbol{Y}^{-1}\boldsymbol{y})\cdot\boldsymbol{Y}\cdot(\boldsymbol{n}+\boldsymbol{Y}^{-1}\boldsymbol{y})+-\frac{1}{2}\boldsymbol{y}\cdot\boldsymbol{Y}^{-1}\cdot\boldsymbol{y}\right)} \\
&= e^{\pi\boldsymbol{y}\cdot\boldsymbol{Y}^{-1}\cdot\boldsymbol{y}} \sum_{\boldsymbol{n}\in\mathbb{Z}^g} e^{2\pi i\left(\frac{1}{2}\boldsymbol{n}\cdot\boldsymbol{X}\cdot\boldsymbol{n}+\boldsymbol{n}\cdot\boldsymbol{x}\right)} e^{-\pi\left(\boldsymbol{n}+\boldsymbol{Y}^{-1}\boldsymbol{y}\right)\cdot\boldsymbol{Y}\cdot\left(\boldsymbol{n}+\boldsymbol{Y}^{-1}\boldsymbol{y}\right)} \qquad (2)
\end{aligned}$$

At this point, all exponential growth has been isolated: the factor multiplying the sum grows double-exponentially as the components of $\boldsymbol{z}$ leave the real line, due to the fact that $\boldsymbol{Y}^{-1}$ is strictly positive definite: this follows since $\boldsymbol{Y}$ is strictly positive definite, which also guarantees the existence of $\boldsymbol{Y}^{-1}$. All terms remaining in the sum are either oscillating (the first factor of every term), or a damped exponential (the second factor of every term).

Since for most applications, the exponential growth term cancels out, it will be disregarded in almost all that follows: **any statements of approximation, pointwise or uniform, of the Riemann theta function pertain to the infinite sum in (2), without considering the exponential growth**.

Let $[\boldsymbol{V}]$ be the vector with integer component closest to $\boldsymbol{V}$, and let $[[\boldsymbol{V}]] = \boldsymbol{V} - [\boldsymbol{V}]$. Continuing the rewriting of the theta function,

$$\begin{aligned}
\theta(\boldsymbol{z}|\boldsymbol{\Omega}) &= e^{\pi\boldsymbol{y}\cdot\boldsymbol{Y}^{-1}\cdot\boldsymbol{y}} \sum_{\boldsymbol{n}\in\mathbb{Z}^g} e^{2\pi i\left(\frac{1}{2}\boldsymbol{n}\cdot\boldsymbol{X}\cdot\boldsymbol{n}+\boldsymbol{n}\cdot\boldsymbol{x}\right)} e^{-\pi\left(\boldsymbol{n}+\left[\boldsymbol{Y}^{-1}\boldsymbol{y}\right]+\left[\left[\boldsymbol{Y}^{-1}\boldsymbol{y}\right]\right]\right)\cdot\boldsymbol{Y}\cdot\left(\boldsymbol{n}+\left[\boldsymbol{Y}^{-1}\boldsymbol{y}\right]+\left[\left[\boldsymbol{Y}^{-1}\boldsymbol{y}\right]\right]\right)} \\
&= e^{\pi\boldsymbol{y}\cdot\boldsymbol{Y}^{-1}\cdot\boldsymbol{y}} \sum_{\boldsymbol{n}\in\mathbb{Z}^g} e^{2\pi i\left(\frac{1}{2}\left(\boldsymbol{n}-\left[\boldsymbol{Y}^{-1}\boldsymbol{y}\right]\right)\cdot\boldsymbol{X}\cdot\left(\boldsymbol{n}-\left[\boldsymbol{Y}^{-1}\boldsymbol{y}\right]\right)+\left(\boldsymbol{n}-\left[\boldsymbol{Y}^{-1}\boldsymbol{y}\right]\right)\cdot\boldsymbol{x}\right)} \times \\
&\qquad \times e^{-\pi\left(\boldsymbol{n}+\left[\left[\boldsymbol{Y}^{-1}\boldsymbol{y}\right]\right]\right)\cdot\boldsymbol{Y}\cdot\left(\boldsymbol{n}+\left[\left[\boldsymbol{Y}^{-1}\boldsymbol{y}\right]\right]\right)}. \qquad (3)
\end{aligned}$$

The last step is achieved by shifting the summation index $\boldsymbol{n}$. From this formulation, it is clear that the size of each one of the terms in the infinite sum is controlled by its second exponential factor.

Similarly, formulae are worked out for the derivatives of theta functions. Denote the N-th order directional derivative of the g-variable Riemann theta function along the g-dimensional vectors $\boldsymbol{k}^{(1)}$, …, $\boldsymbol{k}^{(N)}$ as

$$D(\boldsymbol{k}^{(1)},\ldots,\boldsymbol{k}^{(N)})\theta(\boldsymbol{z}|\boldsymbol{\Omega}) = \sum_{i_1,\ldots,i_N=1}^{g} \boldsymbol{k}_{i_1}^{(1)}\ldots\boldsymbol{k}_{i_N}^{(N)} \frac{\partial^N\theta(\boldsymbol{z}|\boldsymbol{\Omega})}{\partial z_{i_1}\ldots\partial z_{i_N}}. \tag{4}$$

Then

$$\begin{aligned} D(\boldsymbol{k}^{(1)},\ldots,\boldsymbol{k}^{(N)})\theta(\boldsymbol{z}|\boldsymbol{\Omega}) &= (2\pi i)^N \sum_{\boldsymbol{n}\in\mathbb{Z}^g} (\boldsymbol{k}^{(1)}\cdot\boldsymbol{n})\ldots(\boldsymbol{k}^{(N)}\cdot\boldsymbol{n}) e^{2\pi i\left(\frac{1}{2}\boldsymbol{n}\cdot\boldsymbol{\Omega}\cdot\boldsymbol{n}+\boldsymbol{n}\cdot\boldsymbol{z}\right)} \\ &= (2\pi i)^N e^{\pi\boldsymbol{y}\cdot\boldsymbol{Y}^{-1}\cdot\boldsymbol{y}} \sum_{\boldsymbol{n}\in\mathbb{Z}^g} \Big(\boldsymbol{k}^{(N)}\cdot\big(\boldsymbol{n}-\big[\boldsymbol{Y}^{-1}\boldsymbol{y}\big]\big)\Big)\ldots\Big(\boldsymbol{k}^{(N)}\cdot\big(\boldsymbol{n}-\big[\boldsymbol{Y}^{-1}\boldsymbol{y}\big]\big)\Big)\times \\ &\quad\times e^{2\pi i\left(\frac{1}{2}\left(\boldsymbol{n}-\left[\boldsymbol{Y}^{-1}\boldsymbol{y}\right]\right)\cdot\boldsymbol{X}\cdot\left(\boldsymbol{n}-\left[\boldsymbol{Y}^{-1}\boldsymbol{y}\right]\right)+\left(\boldsymbol{n}-\left[\boldsymbol{Y}^{-1}\boldsymbol{y}\right]\right)\cdot\boldsymbol{x}\right)}\times \\ &\quad\times e^{-\pi\left(\boldsymbol{n}+\left[\left[\boldsymbol{Y}^{-1}\boldsymbol{y}\right]\right]\right)\cdot\boldsymbol{Y}\cdot\left(\boldsymbol{n}+\left[\left[\boldsymbol{Y}^{-1}\boldsymbol{y}\right]\right]\right)}, \end{aligned} \tag{5}$$

using similar steps as before. The exponential growth is still factored out, but the remaining infinite sum now contains terms that grow algebraically as the argument of the Riemann theta function leaves the real line. The order of this growth is equal to the order of the derivative. However, the size of individual terms within the infinite sum is again determined by the last factor which is exponentially decaying.

Remark. Riemann theta functions of genus greater than one have been computed before, for instance in [8], where genus three was considered. There four distinct representations of these Riemann theta functions were used, based on whether the different phases behaved as trigonometric or hyperbolic functions (two limits of elliptic functions), depending on the parameters in the Riemann matrix. These distinct representations were required to have a manageable number of contributing terms to the series. Such a variety of representations is not needed here: all limit cases are incorporated in the form (3). This is obtained by the separation of the real and imaginary parts of both the argument $\boldsymbol{z}$ and the Riemann matrix $\boldsymbol{\Omega}$.

4 Pointwise Approximation

The formulae (3) and (5) are the basis for the approximation of theta functions and their derivatives. All approximations are based on determining which terms of the infinite sum are dominant.

For the Riemann theta function,

$$\begin{aligned} \theta(\boldsymbol{z}|\boldsymbol{\Omega})e^{-\pi\boldsymbol{y}\cdot\boldsymbol{Y}^{-1}\cdot\boldsymbol{y}} &= \sum_{\boldsymbol{n}\in\mathbb{Z}^g} e^{2\pi i\left(\frac{1}{2}\left(\boldsymbol{n}-\left[\boldsymbol{Y}^{-1}\boldsymbol{y}\right]\right)\cdot\boldsymbol{X}\cdot\left(\boldsymbol{n}-\left[\boldsymbol{Y}^{-1}\boldsymbol{y}\right]\right)+\left(\boldsymbol{n}-\left[\boldsymbol{Y}^{-1}\boldsymbol{y}\right]\right)\cdot\boldsymbol{x}\right)}\times \\ &\quad\times e^{-\pi\left(\boldsymbol{n}+\left[\left[\boldsymbol{Y}^{-1}\boldsymbol{y}\right]\right]\right)\cdot\boldsymbol{Y}\cdot\left(\boldsymbol{n}+\left[\left[\boldsymbol{Y}^{-1}\boldsymbol{y}\right]\right]\right)} \end{aligned}$$

$$= \lim_{R\to\infty} \sum_{S_R} e^{2\pi i\left(\frac{1}{2}\left(\boldsymbol{n}-\left[\boldsymbol{Y}^{-1}\boldsymbol{y}\right]\right)\cdot\boldsymbol{X}\cdot\left(\boldsymbol{n}-\left[\boldsymbol{Y}^{-1}\boldsymbol{y}\right]\right)+\left(\boldsymbol{n}-\left[\boldsymbol{Y}^{-1}\boldsymbol{y}\right]\right)\cdot\boldsymbol{x}\right)} \times$$

$$\times\, e^{-\pi\left(\boldsymbol{n}+\left[\left[\boldsymbol{Y}^{-1}\boldsymbol{y}\right]\right]\right)\cdot\boldsymbol{Y}\cdot\left(\boldsymbol{n}+\left[\left[\boldsymbol{Y}^{-1}\boldsymbol{y}\right]\right]\right)}, \tag{6}$$

where

$$S_R = \left\{\boldsymbol{n}\in\mathbb{Z}^g | \pi\left(\boldsymbol{n}+\left[\left[\boldsymbol{Y}^{-1}\boldsymbol{y}\right]\right]\right)\cdot\boldsymbol{Y}\cdot\left(\boldsymbol{n}+\left[\left[\boldsymbol{Y}^{-1}\boldsymbol{y}\right]\right]\right) < R^2\right\}. \tag{7}$$

Below, we show this limit exists, hence proving that the Riemann theta function is well defined. This proof is different from that found in many references (see [14], for example) in that it also allows the estimation of the error made in the approximation of the truncation of the series by only considering a finite value of R.

Since $\boldsymbol{Y}$ is strictly positive definite, it has a Cholesky decomposition, $\boldsymbol{Y} = \boldsymbol{T}^T\boldsymbol{T}$. Let Λ be the lattice of all vectors $\boldsymbol{v}(\boldsymbol{n})$ of the form $\boldsymbol{v}(\boldsymbol{n}) = \sqrt{\pi}\boldsymbol{T}\left(\boldsymbol{n}+\left[\left[\boldsymbol{Y}^{-1}\boldsymbol{y}\right]\right]\right)$, for $\boldsymbol{n}\in\mathbb{Z}^g$. Then S_R is rewritten as

$$S_R = \left\{\boldsymbol{v}(\boldsymbol{n})\in\Lambda\middle| ||\boldsymbol{v}(\boldsymbol{n})|| < R\right\}. \tag{8}$$

Thus, the approximation requires finding all lattice points in Λ that are also inside the g-dimensional sphere $||v(n)|| = R$.
Let

$$\theta_R(\boldsymbol{z}|\boldsymbol{\Omega}) = e^{\pi\boldsymbol{y}\cdot\boldsymbol{Y}^{-1}\cdot\boldsymbol{y}}\sum_{S_R} e^{2\pi i\left(\frac{1}{2}\left(\boldsymbol{n}-\left[\boldsymbol{Y}^{-1}\boldsymbol{y}\right]\right)\cdot\boldsymbol{X}\cdot\left(\boldsymbol{n}-\left[\boldsymbol{Y}^{-1}\boldsymbol{y}\right]\right)+\left(\boldsymbol{n}-\left[\boldsymbol{Y}^{-1}\boldsymbol{y}\right]\right)\cdot\boldsymbol{x}\right)} e^{-||\boldsymbol{v}(\boldsymbol{n})||^2}, \tag{9}$$

then

$$\begin{aligned}
\epsilon(R) &= |\theta(\boldsymbol{z}|\boldsymbol{\Omega}) - \theta_R(\boldsymbol{z}|\boldsymbol{\Omega})|\, e^{-\pi\boldsymbol{y}\cdot\boldsymbol{Y}^{-1}\cdot\boldsymbol{y}} && (10)\\
&= \left|\sum_{\Lambda\setminus S_R} e^{2\pi i\left(\frac{1}{2}\left(\boldsymbol{n}-\left[\boldsymbol{Y}^{-1}\boldsymbol{y}\right]\right)\cdot\boldsymbol{X}\cdot\left(\boldsymbol{n}-\left[\boldsymbol{Y}^{-1}\boldsymbol{y}\right]\right)+\left(\boldsymbol{n}-\left[\boldsymbol{Y}^{-1}\boldsymbol{y}\right]\right)\cdot\boldsymbol{x}\right)} e^{-||\boldsymbol{v}(\boldsymbol{n})||^2}\right| \\
&\le \sum_{\Lambda\setminus S_R}\left|e^{2\pi i\left(\frac{1}{2}\left(\boldsymbol{n}-\left[\boldsymbol{Y}^{-1}\boldsymbol{y}\right]\right)\cdot\boldsymbol{X}\cdot\left(\boldsymbol{n}-\left[\boldsymbol{Y}^{-1}\boldsymbol{y}\right]\right)+\left(\boldsymbol{n}-\left[\boldsymbol{Y}^{-1}\boldsymbol{y}\right]\right)\cdot\boldsymbol{x}\right)} e^{-||\boldsymbol{v}(\boldsymbol{n})||^2}\right| \\
&= \sum_{\Lambda\setminus S_R} e^{-||\boldsymbol{v}(\boldsymbol{n})||^2}. && (11)
\end{aligned}$$

Thus $\epsilon(R)$ is the absolute error of the oscillatory part of the Riemann theta function, due to the truncation to a finite number of terms. In practice, this oscillatory part is of order 1, so $\epsilon(R)$ is also a measure of the relative error.

In order to estimate this last sum, the following theorems and lemmas are used.

Theorem 1 (Mean-value Theorem for subharmonic functions) *Let Ω be a domain in $\mathbb{R}^g$. Let u be a twice continuously differentiable function on Ω, continuous on the boundary of $\partial\Omega$ of Ω, which is subharmonic on Ω. Then for any ball $B_R^g(\boldsymbol{y})$ in Ω of radius R and center $\boldsymbol{y}$*

$$u(\boldsymbol{y}) \le \frac{1}{R^g \mathrm{Vol}B_1^g(0)}\int_{B_R^g(\boldsymbol{y})} u(\boldsymbol{x})d\boldsymbol{x}. \tag{12}$$

A proof of this theorem is found in [9].

Lemma 1 *For every integer $p \geq 0$ and any dimension $g > 0$ the function $u(\boldsymbol{y}) = e^{-||\boldsymbol{y}||^2}||\boldsymbol{y}||^p$ with $\boldsymbol{y} \in \mathbb{R}^g$ is subharmonic on $\mathbb{R}^g \setminus B_R^g(0)$, with $R = \frac{1}{2}\sqrt{g + 2p + \sqrt{g^2 + 8p}}$.*

Proof. Since $u(\boldsymbol{y})$ depends only on $r = ||\boldsymbol{y}||$, this calculation is done in g-dimensional spherical coordinates.

$$\begin{aligned} \Delta u(\boldsymbol{y}) &= \frac{\partial^2 u}{\partial r^2} + \frac{g-1}{r}\frac{\partial u}{\partial r} \\ &= 2u(\boldsymbol{y})\left(2r^2 - (g+2p) + \frac{p^2 + (g-2)p}{2r^2}\right) \end{aligned}$$

This last factor is positive if $r > \frac{1}{2}\sqrt{g + 2p + \sqrt{g^2 + 8p}}$, from which the result follows. ■

Lemma 2 *Let Λ be a g-dimensional affine lattice in $\mathbb{R}^g$, i.e., $\Lambda = \{\boldsymbol{X}\boldsymbol{n} + \boldsymbol{x} | \boldsymbol{n} \in \mathbb{Z}^g\}$, with $\boldsymbol{X} \in Gl(n, \mathbb{R})$, $\boldsymbol{x} \in \mathbb{R}^g$, and let $p \in \mathbb{Z}$, positive. Then*

$$\sum_{\boldsymbol{y}\in\Lambda, ||\boldsymbol{y}|| \geq R} ||\boldsymbol{y}||^p e^{-||\boldsymbol{y}||^2} \leq \frac{g}{2}\left(\frac{2}{\rho}\right)^g \Gamma\left(\frac{g+p}{2}, (R - \rho/2)^2\right), \tag{13}$$

where $\Gamma(z, d) = \int_d^\infty t^{z-1}e^{-z}dz$, the incomplete Gamma function [1], $R > \frac{1}{2}\sqrt{g + 2p + \sqrt{g^2 + 8p}} + \rho/2$, and $\rho = \min\{||\boldsymbol{x} - \boldsymbol{y}|| \ | \boldsymbol{x}, \boldsymbol{y} \in \Lambda, \boldsymbol{x} \neq \boldsymbol{y}\}$.

Proof. By the previous lemmas,

$$\begin{aligned} \sum_{\boldsymbol{y}\in\Lambda, ||\boldsymbol{y}|| \geq R} ||\boldsymbol{y}||^p e^{-||\boldsymbol{y}||^2} &\leq \sum_{\boldsymbol{y}\in\Lambda, ||\boldsymbol{y}|| \geq R} \frac{1}{(\rho/2)^g \mathrm{Vol}B_1^g(0)} \int_{B^g_{\rho/2}(\boldsymbol{y})} ||\boldsymbol{x}||^p e^{-||\boldsymbol{x}||^2} d\boldsymbol{x} \\ &= \frac{1}{\mathrm{Vol}B_1^g(0)}\left(\frac{2}{\rho}\right)^g \sum_{\boldsymbol{y}\in\Lambda, ||\boldsymbol{y}|| \geq R} \int_{B^g_{\rho/2}(\boldsymbol{y})} ||\boldsymbol{x}||^p e^{-||\boldsymbol{x}||^2} d\boldsymbol{x} \qquad (14) \\ &\leq \frac{1}{\mathrm{Vol}B_1^g(0)}\left(\frac{2}{\rho}\right)^g \int_{\mathbb{R}^g \setminus B^g_{R-\rho/2}(0)} ||\boldsymbol{x}||^p e^{-||\boldsymbol{x}||^2} d\boldsymbol{x} \\ &= \frac{\mathrm{Vol}S_1^{g-1}(0)}{\mathrm{Vol}B_1^g(0)}\left(\frac{2}{\rho}\right)^g \int_{R-\rho/2}^\infty e^{-r^2} r^{g-1+p} dr \\ &= \frac{g}{2}\left(\frac{2}{\rho}\right)^g \int_{(R-\rho/2)^2}^\infty e^{-t} t^{(g+p)/2-1} dt \\ &= \frac{g}{2}\left(\frac{2}{\rho}\right)^g \Gamma\left(\frac{g+p}{2}, (R-\rho/2)^2\right). \end{aligned}$$

Here $\mathrm{Vol}S_r^{g-1}(0)/\mathrm{Vol}V_r^g(0) = g/r$ was used. ■

Remark. The inequality following (14) is quite crude. Specifically, it adds all the space in between the balls around the lattice points. Taking this in to account, another estimate is as

follows:

$$\begin{aligned}\sum_{\boldsymbol{y}\in\Lambda,||\boldsymbol{y}||\geq R}||\boldsymbol{y}||^p e^{-||\boldsymbol{y}||^2} &\leq \frac{1}{\mathrm{Vol}B_1^g(0)}\left(\frac{2}{\rho}\right)^g \sum_{\boldsymbol{y}\in\Lambda,||\boldsymbol{y}||\geq R}\int_{B^g_{\rho/2}(\boldsymbol{y})}||\boldsymbol{x}||^p e^{-||\boldsymbol{x}||^2}d\boldsymbol{x} \\ &\approx \frac{1}{\mathrm{Vol}B_1^g(0)}\left(\frac{2}{\rho}\right)^g c(\Lambda,\rho/2)\int_{\mathbb{R}^g\setminus B^g_{R-\rho/2}(0)}||\boldsymbol{x}||^p e^{-||\boldsymbol{x}||^2}d\boldsymbol{x}.\end{aligned}$$

Here $c(\Lambda,\rho/2)$ is the "fill factor" of the lattice Λ with balls of radius $\rho/2$: it is the fraction of the lattice volume that is filled if a ball of radius $\rho/2$ is placed at every lattice point. This estimate is justified, since the function being integrated only depends on the radial variable. Thus, within thin radial shells the function is almost constant, independent of the proximity to a lattice point. The crudeness of the inequality following (14) is illustrated in Fig. 1, where the fill factor $c(\Lambda,\rho/2)$ is shown for the scenario of minimal $|\Lambda| = \rho^g$, *i.e.*, a square lattice. Then $c(\Lambda,\rho/2) = \pi^{g/2}/(2^{g-1}g\Gamma(g/2))$, which decays fast as $g\to\infty$. Figure 1 shows that for a square lattice, not using the fill factor results in the error being overestimated by only one digit for $g = 6$. Using the fill factor for generic lattices, where $\Lambda > \rho^g$, usually leads to a more significant improvement.

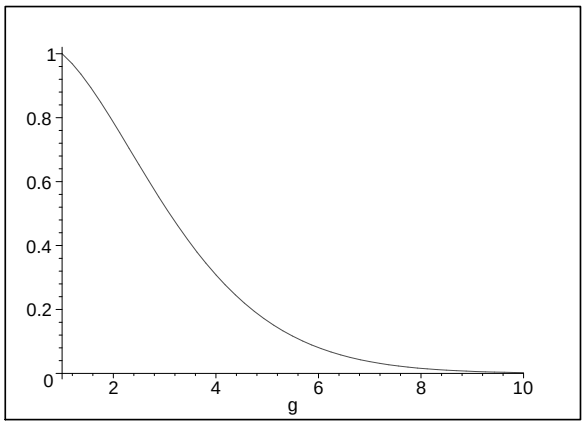

Figure 1: Fill factor $c(\Lambda,\rho/2)$ for the case of a square lattice.

Thus $c(\Lambda,\rho/2) = \mathrm{Vol}B^g_{\rho/2}(0)/|\Lambda| = \dfrac{2\pi^{g/2}}{g\Gamma(g/2)}\dfrac{(\rho/2)^g}{|\Lambda|}$, where $|\Lambda|$ is the determinant of the lattice. It is the volume of a cell of Λ spanned by a set of generating vectors. This gives

$$\begin{aligned}\sum_{\boldsymbol{y}\in\Lambda,||\boldsymbol{y}||\geq R}||\boldsymbol{y}||^p e^{-||\boldsymbol{y}||^2} &\lessapprox \frac{\mathrm{Vol}S_1^{g-1}(0)}{\mathrm{Vol}B_1^g(0)}\left(\frac{2}{\rho}\right)^g \frac{2\pi^{g/2}}{g\Gamma(g/2)}\frac{(\rho/2)^g}{|\Lambda|}\int_{R-\rho/2}^{\infty} e^{-r^2}r^{g-1+p}dr \\ &= g\frac{2\pi^{g/2}}{g\Gamma(g/2)}\frac{1}{|\Lambda|}\frac{1}{2}\int_{(R-\rho/2)^2}^{\infty} e^{-t}t^{(g+p)/2-1}dt \\ &= \frac{\pi^{g/2}}{|\Lambda|\Gamma(g/2)}\Gamma\left(\frac{g+p}{2},(R-\rho/2)^2\right). \qquad (15)\end{aligned}$$

Using (13) with $p = 0$, (11) becomes

$$\epsilon(R) \leq \sum_{\Lambda \backslash S_R} e^{-||\boldsymbol{v}(\boldsymbol{n})||^2} \leq \frac{g}{2} \left(\frac{2}{\rho}\right)^g \Gamma\left(\frac{g}{2}, (R-\rho/2)^2\right), \tag{16}$$

where ρ is the length of the shortest lattice vector in Λ: $\rho = \min\{||x||, x \in \Lambda\}$, and $R > (\sqrt{2g}+\rho)/2$ (to satisfy the subharmonicity condition of Lemma 1). As claimed, this proves that the Riemann theta function is well-defined, since $\lim_{R\to\infty} \Gamma(z, R) = 0$ [1].

Thus, in order to approximate the oscillatory part of a Riemann theta function of g complex variables with a pre-determined error ϵ, one solves the equation

$$\epsilon = \frac{g}{2} \left(\frac{2}{\rho}\right)^g \Gamma\left(\frac{g}{2}, (R-\rho/2)^2\right), \tag{17}$$

for R, with $R > (\sqrt{2g}+\rho)/2$, real. If no solution exists, then $R = (\sqrt{2g}+\rho)/2$ suffices. These results combine to give

Theorem 2 (Pointwise Approximation) *The Riemann theta function is approximated by*

$$\theta(\boldsymbol{z}|\boldsymbol{\Omega}) \approx e^{\pi \boldsymbol{y}\cdot\boldsymbol{Y}^{-1}\cdot\boldsymbol{y}} \sum_{S_R} e^{2\pi i\left(\frac{1}{2}\left(\boldsymbol{n}-\left[\boldsymbol{Y}^{-1}\boldsymbol{y}\right]\right)\cdot\boldsymbol{X}\cdot\left(\boldsymbol{n}-\left[\boldsymbol{Y}^{-1}\boldsymbol{y}\right]\right)+\left(\boldsymbol{n}-\left[\boldsymbol{Y}^{-1}\boldsymbol{y}\right]\right)\cdot\boldsymbol{x}\right)} e^{-||\boldsymbol{v}(\boldsymbol{n})||^2}, \tag{18}$$

with absolute error ϵ on the sum. Here $S_R = \{\boldsymbol{v}(\boldsymbol{n}) \in \Lambda |\ ||\boldsymbol{v}(n)|| < R\}$, $\Lambda = \left\{\sqrt{\pi}\boldsymbol{T}(\boldsymbol{n} + [[\boldsymbol{Y}^{-1}\boldsymbol{y}]]) \ |\boldsymbol{n} \in \mathbb{Z}^g\right\}$. The shortest distance between any two points of Λ is denoted by ρ. Then the radius R is determined as the greater of $(\sqrt{2g}+\rho)/2$ and the real positive solution of $\epsilon = g\, 2^{g-1}\Gamma\left(g/2, (R-\rho/2)^2\right)/\rho^g$.

This theorem gives a pointwise approximation to the Riemann theta function: for every $\boldsymbol{z}$ at which the Riemann theta function is approximated, S_R is different, although R is unchanged as long as g and ϵ remain the same. The error used in Theorem 2 is referred to as the 100% Error (100%E).

Another good estimate for R is obtained from (15). Then R is the greater of $(\sqrt{2g}+\rho)/2$ and the real positive solution of $\epsilon = \pi^{g/2}\Gamma\left(g/2, (R-\rho/2)^2\right)/(|\Lambda|\Gamma(g/2))$. This error is referred to as the Fill Factor Error (FFE).

Figure 2 compares the size R of the ellipsoid, required to obtain a prescribed error ϵ, as a result of using the 100%E or the FFE, for the cases $g = 2$ and $g = 16$. In these figures, the worst-case scenario $|\Lambda| = \rho^g$ was assumed. As expected, the difference between the 100%E and the FFE is small for small genus, but becomes significant for larger genus.

Two examples are shown in Table 1, for various values of ϵ. Both of these use the Riemann matrix $\boldsymbol{\Omega}_g$ with $\Omega_{jj} = i$, $j = 1, \ldots, g$, and $\Omega_{jk} = -1/2$, $j \neq k$. The first example (left side of the table) corresponds to $g = 2$, the second (right side) to $g = 6$. For both examples, the Riemann theta function is evaluated at $\boldsymbol{z} = \boldsymbol{0}$, thus in this case the oscillatory part of the Riemann theta function equals the Riemann theta function. The value of the Riemann theta function is given in the first line. The first column of an example gives ϵ, used for the pointwise approximation, with either the 100%E, or the FFE. In the table N(100%E) and N(FFE) denote the number of terms that are used

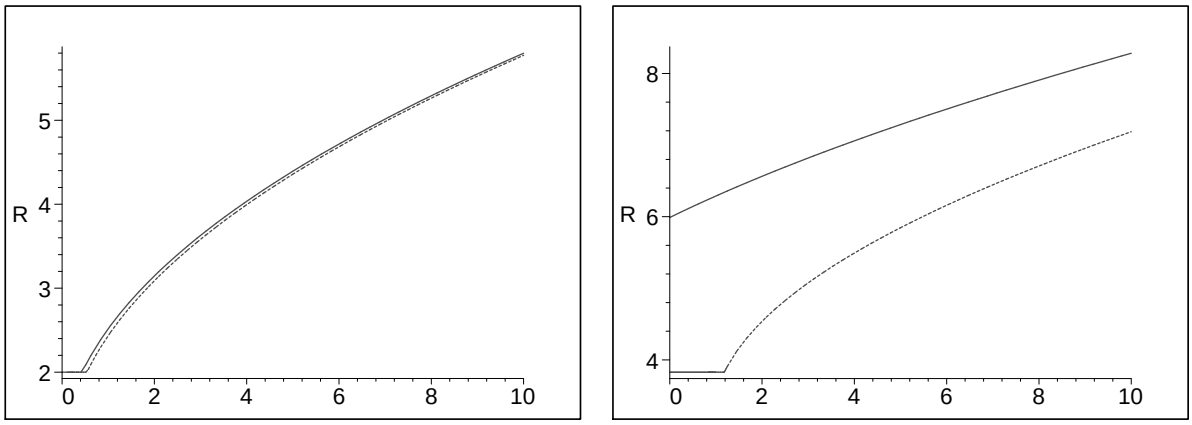

(a) $g = 2$ (b) $g = 16$

Figure 2: R, assuming the 100% Error (solid line) and Fill Factor Error (dashed line) as functions of $-log_{10}(\epsilon)$, which is the number of accurate digits.

to compute the oscillatory part of the Riemann theta function, *i.e.*, the number of elements of S_R, using the 100%E or the FFE, respectively. AE denotes Actual Error, *i.e.*, the difference between the actual value of the oscillatory part of the Riemann theta function (computed using 30 digits of accuracy, and $\epsilon = 10^{-30}$) and the computed value, using the two different error formulae.

Using (3), we see that the first example, with $g = 2$, computes $\sum_{n_1,n_2=-\infty}^{\infty} \cos(n_1 n_2 \pi) e^{-\pi(n_1^2+n_2^2)}$. Since for this example $g = 2$, there should be little difference between the computation using the 100%E or the FFE. This is confirmed: although the value of R is slightly different for both computations, the number of elements of S_R is identical, resulting in both computations having the same accuracy.

For the second example, with $g = 6$, there is a difference between the two computations, although it is not as outspoken as for $g = 16$ in Fig. 2. It is clear that the Actual Error using the FFE computation is closer to ϵ, than using the 100%E. Even in this case, the computation does several orders of magnitude better than prescribed. This, of course, is due to the inequalities that were used to obtain these error estimates.

Remarks

- The method for approximating the oscillatory part of a Riemann theta function requires the determination of the elements of S_R. This is the set of all elements of Λ that lie inside the g-dimensional sphere determined by $||v(n)|| = R$. It is easier to consider the equivalent problem of determining the points with integer coordinates that lie inside the g-dimensional ellipsoid determined by $\pi(\boldsymbol{n} - \boldsymbol{c}) \cdot \boldsymbol{Y} \cdot (\boldsymbol{n} - \boldsymbol{c}) = R^2$, where c is the center of the ellipsoid. This is done recursively, by remarking that every $(g-1)$-dimensional plane section of a g-dimensional ellipsoid is a $(g-1)$-dimensional sphere. A finite number (due to the discrete nature of the lattice) of such $(g-1)$-dimensional sections are taken. All of these are $(g-1)$-dimensional ellipsoids, on which this section process is repeated, until one arrives at a one-dimensional ellipsoid, *i.e.*, a line piece. At this level it is easy to determine which integer points are in this

$g=2$ $\theta(0,0\|\boldsymbol{\Omega_2})\, e^{-\pi \boldsymbol{y}\cdot\boldsymbol{Y}_2^{-1}\boldsymbol{y}} = 1.1654010572$			$g=6$ $\theta(0,0,0,0,0,0\|\boldsymbol{\Omega_6})\, e^{-\pi \boldsymbol{y}\cdot\boldsymbol{Y}_6^{-1}\boldsymbol{y}} = 8.3721839831$				
ϵ	N(100%E) $= N$(FFE)	AE(100%FE) =AE(FFE)	ϵ	N(100%E)	AE(100%FE)	N(FFE)	AE(FFE)
1E-1	5	7.5E-3	1E-1	485	4.3E-5	233	9.2E-4
1E-2	9	1.5E-5	1E-2	797	3.8E-6	485	4.3E-5
1E-3	13	1.2E-6	1E-3	1341	2.6E-7	797	3.8E-6
1E-4	21	5.1E-11	1E-4	2301	1.3E-8	1341	2.6E-7
1E-5	21	5.1E-11	1E-5	3321	4.2E-10	2301	1.3E-8
1E-6	21	5.1E-11	1E-6	4197	3.8E-11	3321	4.2E-10
1E-7	21	5.1E-11	1E-7	5757	2.3E-12	4197	3.8E-11
1E-8	25	1.9E-12	1E-8	8157	9.2E-14	5757	2.3E-12
1E-9	29	1.8E-13	1E-9	10237	3.5E-15	8157	9.2E-14
1E-10	37	1.5E-17	1E-10	12277	2.7E-16	10237	3.5E-15

Table 1: Two examples of using the pointwise approximation to compute the oscillatory part of a Riemann theta function.

piece. This method takes full advantage of the triangular form of the Cholesky decomposition of $\boldsymbol{Y} = \boldsymbol{T}^T\boldsymbol{T}$. This is done as follows: all integer points satisfying

$$\|\boldsymbol{T}(\boldsymbol{n}-\boldsymbol{c})\| < R/\sqrt{\pi} \tag{19}$$

are sought for. Since $\boldsymbol{T}$ is upper triangular, this implies $|T_{gg}(n_g - c_g)| < R/\sqrt{\pi}$, or

$$c_g - \frac{R}{\sqrt{\pi}T_{gg}} < n_g < c_g + \frac{R}{\sqrt{\pi}T_{gg}}.$$

This gives a set of allowed values of n_g. For each one of these, write $\boldsymbol{n} = (\hat{\boldsymbol{n}}, n_g)^T$, $\boldsymbol{c} = (\hat{\boldsymbol{c}}, c_g)^T$. With

$$\boldsymbol{T} = \begin{pmatrix} \hat{\boldsymbol{T}} & \hat{\boldsymbol{t}} \\ \boldsymbol{0} & T_{gg} \end{pmatrix},$$

(19) becomes $\|\hat{\boldsymbol{T}}(\hat{\boldsymbol{n}}-\hat{\boldsymbol{c}}) + \hat{\boldsymbol{t}}(n_g - c_g)\|^2 + T_{gg}^2(n_g-c_g)^2 < R^2/\pi$, which is rewritten as

$$\|\hat{\boldsymbol{T}}(\hat{\boldsymbol{n}}-\hat{\boldsymbol{c}} + \hat{\boldsymbol{T}}^{-1}\hat{\boldsymbol{t}}(n_g-c_g))\| < \sqrt{R^2/\pi - T_{gg}^2(n_g-c_g)^2}$$

This is a similar problem as (19), but in dimension $g-1$ instead of g, and with a different R, $\boldsymbol{c}$ and $\boldsymbol{T}$. The procedure is now repeated.

- Both error estimates require the knowledge of ρ, the shortest lattice vector of Λ. The problem of finding the shortest lattice vector of a given lattice is one of the main problems in the study of lattices. It is usually addressed using lattice reduction. Lattice reduction attempts to find a standard form for the matrix of generating vectors $\boldsymbol{t}_j$, $j = 1, \ldots, g$ of the lattice, in which certain intrinsic (*i.e.*, independent of the representation of the generating vectors; such as ρ, for instance) properties of the lattice are easier to examine. The problem of computing ρ is

known to be NP hard in the parameters g and $\ln(\max_j(||t_j||))$ [19]. However, an approximate algorithm due to Lenstra, Lenstra and Lovász (the LLL algorithm, [13]) is known which is polynomially hard in g and $\ln(\max_j(||t_j||))$. This approximate algorithm is exact in low dimensions (guaranteed in 1,2 and 3), but only gives approximate answers in high dimensions. In practice, the algorithm has been found very satisfactory. A rigorous error estimation is possible using the results of the LLL algorithm, as it provides both a lower and an upper bound for ρ: If $\hat{\rho}$ is the value of ρ found by the LLL algorithm, then $\hat{\rho}/2^{(g-1)/2} \leq \rho \leq \hat{\rho}$. Since the LLL algorithm for relatively low genera ($g < 10$) usually finds the correct value of ρ, this will not be pursued here.

5 Uniform Approximation

It is now easy to extend the results of the previous section to obtain results for the uniform approximation of the oscillatory part of Riemann theta functions. In Theorem 2, the sum extends over all terms whose summation index vector is inside an ellipsoid. The size of this ellipsoid (R) is determined by the allowed error of the pointwise approximation. The shape of the ellipsoid depends on $\mathbf{\Omega}$, but not on $\boldsymbol{z}$. The center of the ellipsoid is $-[[\boldsymbol{Y}^{-1}\boldsymbol{y}]]$. So, if different arguments $\boldsymbol{z}$ are considered, only the center of the ellipsoid changes and not its shape or size. But, this center can only wander over a g-dimensional cube of volume 1, centered around the origin. This leads to the following

Theorem 3 (Uniform Approximation) *The Riemann theta function is approximated by*

$$\theta(\boldsymbol{z}|\mathbf{\Omega}) \approx e^{\pi \boldsymbol{y}\cdot\boldsymbol{Y}^{-1}\cdot\boldsymbol{y}} \sum_{U_R} e^{2\pi i\left(\frac{1}{2}\left(\boldsymbol{n}-\left[\boldsymbol{Y}^{-1}\boldsymbol{y}\right]\right)\cdot\boldsymbol{X}\cdot\left(\boldsymbol{n}-\left[\boldsymbol{Y}^{-1}\boldsymbol{y}\right]\right)+\left(\boldsymbol{n}-\left[\boldsymbol{Y}^{-1}\boldsymbol{y}\right]\right)\cdot\boldsymbol{x}\right)} e^{-||\boldsymbol{v}(\boldsymbol{n})||^2}, \qquad (20)$$

with absolute error ϵ on the sum. The approximation of the sum is uniform in $\boldsymbol{z}$. Here $\boldsymbol{v}(\boldsymbol{n}) = \sqrt{\pi}\boldsymbol{T}(\boldsymbol{n} + [[\boldsymbol{Y}^{-1}\boldsymbol{y}]])$,

$$U_R = \left\{\boldsymbol{n} \in \mathbb{Z}^g | \pi(\boldsymbol{n}-\boldsymbol{c})\cdot\boldsymbol{Y}\cdot(\boldsymbol{n}-\boldsymbol{c}) < R^2, |c_j| < 1/2, j = 1,\ldots,g\right\}. \qquad (21)$$

Let $\Lambda = \left\{\sqrt{\pi}\boldsymbol{T}(\boldsymbol{n} + [[\boldsymbol{Y}^{-1}\boldsymbol{y}]]) \;|\boldsymbol{n} \in \mathbb{Z}^g\right\}$. The shortest distance between any two points of Λ is denoted by ρ. Then the radius R is determined as the greater of $(\sqrt{2g}+\rho)/2$ and the real positive solution of $\epsilon = g\, 2^{g-1}\Gamma\left(g/2, (R-\rho/2)^2\right)/\rho^g$.

Thus, to obtain a uniform in $\boldsymbol{z}$ approximation with absolute error ϵ for the oscillatory part of the Riemann theta function parametrized by $\mathbf{\Omega}$, it suffices to add all terms whose summation index is inside the envelope of all ellipsoids of size R (determined by ϵ) whose shape is determined by $\mathbf{\Omega}$, and whose center is at any point inside the unit cube centered at the origin. This object is also obtained as the convex hull of all ellipsoids of size R placed at all corners of the unit cube centered at the origin. This situation is illustrated in Fig. 3. The ellipsoid on the left illustrates the scenario of obtaining the summation indices for a pointwise approximation. The deformed ellipsoid on the right illustrates the case of a uniform approximation. The deformation is a consequence of the wandering of the center of the ellipsoid over the unit cube.

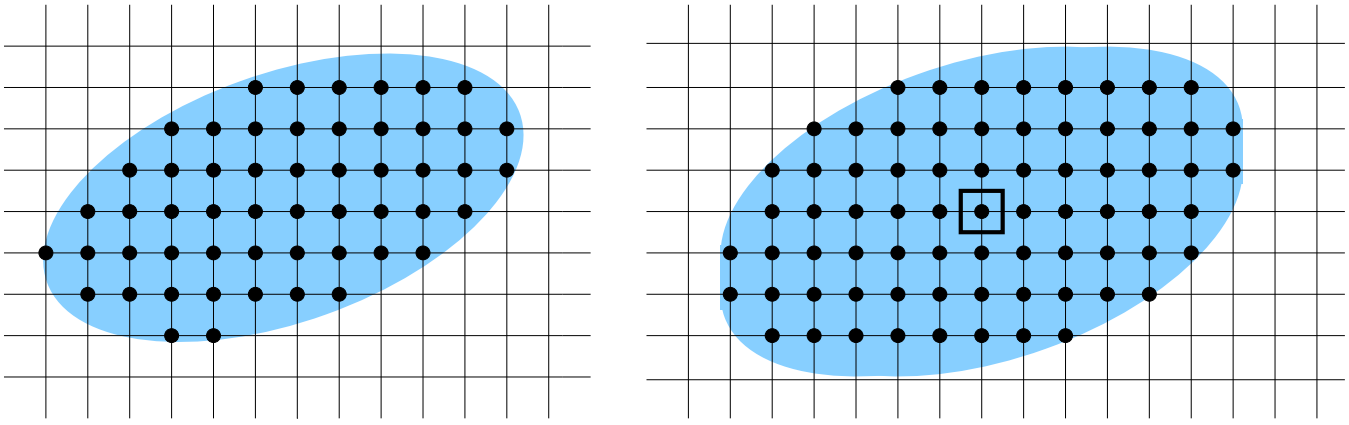

(a) (b)

Figure 3: Summation indices (a) for a pointwise approximation, inside an ellipsoid centered at $[[\boldsymbol{Y}^{-1}\boldsymbol{y}]]$, and (b) for a uniform approximation, inside an ellipsoid whose center moves around the unit cube.

It is clear that using a uniform approximation results in more terms of the sum being used. In many applications (graphics, creation of value tables, *etc.*) many values of the same Riemann theta function (*i.e.*, with constant $\boldsymbol{\Omega}$) are computed. In such cases it is beneficial to use the same representation for the computation.

Remarks

- For the purposes of obtaining a uniform approximation formula, it is essential that the exponential growth was factored out in (3).
- The above theorem uses the 100 % Error of Theorem 2. Just as in the case of a pointwise approximation, it is possible to consider a uniform approximation using a Fill Factor Error. This results in similar modifications to Theorem 3 as for Theorem 2.
- Determining the set U_R is not trivial. In practice, it may be more convenient to work with a single ellipsoid centered at the origin, which is too large.

As an example, consider the Riemann matrix

$$\boldsymbol{\Omega} = \begin{pmatrix} 1.690983006 + 0.9510565162\,i & 1.5 + 0.363271264\,i \\ 1.5 + 0.363271264\,i & 1.309016994 + 0.9510565162\,i \end{pmatrix}. \tag{22}$$

This is the Riemann matrix associated with the genus 2 Riemann surface obtained by compactifying and desingularizing the algebraic curve $\mu^3 - \lambda^7 + 2\lambda^3\mu = 0$. It was computed using the algorithms outlined in [6]. Using the above theorem with $\epsilon = 0.001$, 23 terms have a contribution to the oscillatory part of the Riemann theta function. They have summation indices

$$U_R(100\%E) \quad = \quad \{(-2,2),(2,-2),(0,2),(0,-2),(2,-1),(-2,1),(2,0),(-2,0),(0,-1),$$

$$(0,1),(-1,-1),(1,1),(1,0),(-1,0),(-2,-1),(2,1),(-1,1),(1,-1),$$
$$(0,0),(-1,-2),(1,2),(-1,2),(1,-2)\}\,. \tag{23}$$

Thus a sum of 23 terms suffices to approximate the oscillatory part of the Riemann theta function associated with (22) with an absolute error of $\epsilon = 0.001$. This approximation is valid for all $\boldsymbol{z} = (x_1 + iy_1, x_2 + iy_2)$. These 23 terms should be compared to the 12-17 terms required for a pointwise approximation. The pointwise approximation uses sets of summation indices which are subsets of (23), but these subsets differ depending on the value of $\boldsymbol{z} = (x_1 + iy_1, x_2 + iy_2)$.

Using the FFE, a uniform approximation of the sum is obtained using only nine terms. These have summation indices

$$U_R(FFE) = \{(0,-1),(-1,-1),(1,0),(0,1),(-1,1),(0,0,),(1,-1),(1,1),(-1,0)\}\,.$$

Thus, using the FFE, a sum of only nine terms suffices to approximate the oscillatory part of the Riemann theta function associated with (22) with an absolute error of $\epsilon = 0.001$. These nine terms should be compared to the 3-5 terms required for a pointwise approximation using the FFE.

Either one of these two uniform approximations can be used to graph various slices of the oscillatory part of the Riemann theta function. This is a complex function of four real variables, of which many different slices are possible. Twelve graphs are shown in Fig. 4, using the 9-term uniform approximation with the FFE. Note that the oscillatory part of the Riemann theta function is periodic with period 1 in the real part of all components of $\boldsymbol{z}$. This periodicity is inherited from the Riemann theta function.

6 Derivatives of Riemann theta functions

In this section, approximation results for derivatives of Riemann theta functions are obtained. The results are not as clean as for the Riemann theta function itself: even after removing the exponential growth, algebraic growth terms remain in the sum. The order of the algebraic growth equals the order of the derivative. There is only growth on the imaginary axes of the arguments $\boldsymbol{z}$. Therefore, approximations of the sum with absolute error are bound to be valid only pointwise in $\boldsymbol{z}$. It is possible to obtain uniform approximations in $\boldsymbol{z}$ which are valid in a bounded area of $\mathbb{C}^g$. We give the details for directional derivatives of first and second order. Results for higher-order directional derivatives follow in a similar fashion.

6.1 First-order derivatives

With $N = 1$ and $\boldsymbol{k}^{(1)} = \boldsymbol{k}$, (5) gives

$$\begin{aligned}
& e^{-\pi \boldsymbol{y}\cdot\boldsymbol{Y}^{-1}\cdot\boldsymbol{y}}\, D(\boldsymbol{k})\theta(\boldsymbol{z}|\boldsymbol{\Omega}) \\
= \;& 2\pi i\, \boldsymbol{k}\cdot\sum_{\boldsymbol{n}\in\mathbb{Z}^g}\left(\boldsymbol{n}-\left[\boldsymbol{Y}^{-1}\boldsymbol{y}\right]\right) e^{2\pi i\left(\frac{1}{2}\left(\boldsymbol{n}-\left[\boldsymbol{Y}^{-1}\boldsymbol{y}\right]\right)\cdot\boldsymbol{X}\cdot\left(\boldsymbol{n}-\left[\boldsymbol{Y}^{-1}\boldsymbol{y}\right]\right)+\left(\boldsymbol{n}-\left[\boldsymbol{Y}^{-1}\boldsymbol{y}\right]\right)\right)} e^{-||\boldsymbol{v}(\boldsymbol{n})||^2} \\
= \;& \lim_{R\to\infty} 2\pi i\, \boldsymbol{k}\cdot\sum_{S_R}\left(\boldsymbol{n}-\left[\boldsymbol{Y}^{-1}\boldsymbol{y}\right]\right) e^{2\pi i\left(\frac{1}{2}\left(\boldsymbol{n}-\left[\boldsymbol{Y}^{-1}\boldsymbol{y}\right]\right)\cdot\boldsymbol{X}\cdot\left(\boldsymbol{n}-\left[\boldsymbol{Y}^{-1}\boldsymbol{y}\right]\right)+\left(\boldsymbol{n}-\left[\boldsymbol{Y}^{-1}\boldsymbol{y}\right]\right)\right)} \times \\
& \qquad\qquad \times\, e^{-||\boldsymbol{v}(\boldsymbol{n})||^2}, \qquad (24)
\end{aligned}$$

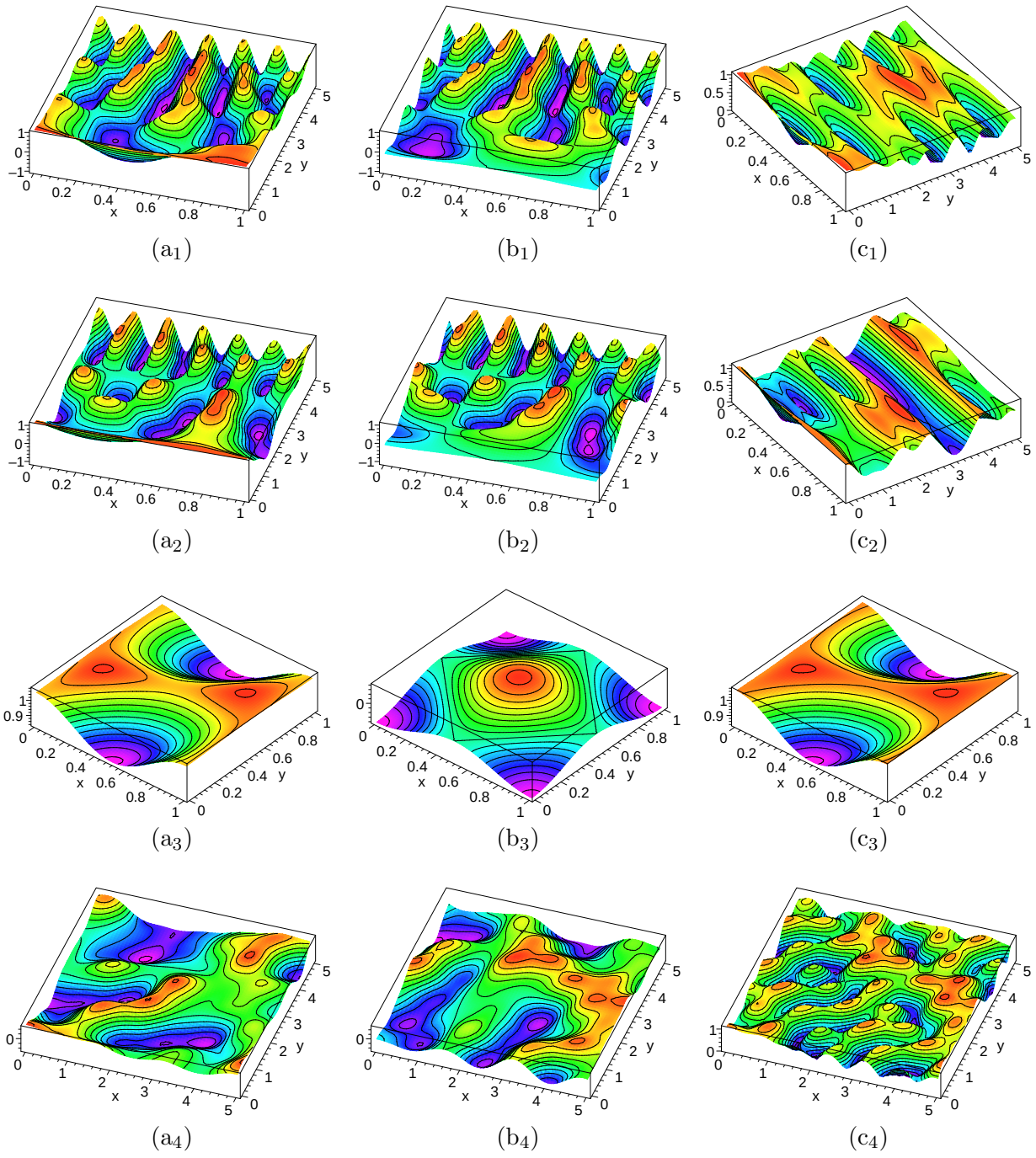

Figure 4: Various views of the oscillatory part of the Riemann theta function parametrized by the Riemann matrix given in (22), with FFE=0.001. All plots are oscillatory parts of $\theta(x+iy,0|\mathbf{\Omega})$ (index 1), $\theta(0,x+iy|\mathbf{\Omega})$ (index 2), $\theta(x,y|\mathbf{\Omega})$ (index 3), $\theta(ix,iy|\mathbf{\Omega})$ (index 4). Shown are the real part (a), the imaginary part (b) and the absolute value (c).

where S_R and $\boldsymbol{v}(\boldsymbol{n})$ are defined as in (8). As before, let

$$D_R(\boldsymbol{k})\theta(\boldsymbol{z}|\boldsymbol{\Omega}) = e^{\pi \boldsymbol{y}\cdot\boldsymbol{Y}^{-1}\cdot\boldsymbol{y}} \times$$
$$\times 2\pi i\, \boldsymbol{k}\cdot\sum_{S_R}\left(\boldsymbol{n}-\left[\boldsymbol{Y}^{-1}\boldsymbol{y}\right]\right) e^{2\pi i\left(\frac{1}{2}\left(\boldsymbol{n}-\left[\boldsymbol{Y}^{-1}\boldsymbol{y}\right]\right)\cdot\boldsymbol{X}\cdot\left(\boldsymbol{n}-\left[\boldsymbol{Y}^{-1}\boldsymbol{y}\right]\right)+\left(\boldsymbol{n}-\left[\boldsymbol{Y}^{-1}\boldsymbol{y}\right]\right)\right)} e^{-||\boldsymbol{v}(\boldsymbol{n})||^2}, \quad (25)$$

then

$$\begin{aligned}
\epsilon(R) &= |D(\boldsymbol{k})\theta(\boldsymbol{z}|\boldsymbol{\Omega}) - D_R(\boldsymbol{k})\theta(\boldsymbol{z}|\boldsymbol{\Omega})|\, e^{\pi \boldsymbol{y}\cdot\boldsymbol{Y}^{-1}\cdot\boldsymbol{y}} \qquad (26)\\
&= \left| 2\pi i\, \boldsymbol{k}\cdot\sum_{\Lambda\setminus S_R}\left(\boldsymbol{n}-\left[\boldsymbol{Y}^{-1}\boldsymbol{y}\right]\right) e^{2\pi i\left(\frac{1}{2}\left(\boldsymbol{n}-\left[\boldsymbol{Y}^{-1}\boldsymbol{y}\right]\right)\cdot\boldsymbol{X}\cdot\left(\boldsymbol{n}-\left[\boldsymbol{Y}^{-1}\boldsymbol{y}\right]\right)+\left(\boldsymbol{n}-\left[\boldsymbol{Y}^{-1}\boldsymbol{y}\right]\right)\right)} e^{-||\boldsymbol{v}(\boldsymbol{n})||^2} \right|\\
&\leq 2\pi||\boldsymbol{k}||\sum_{\Lambda\setminus S_R}\left\|\boldsymbol{n}-\left[\boldsymbol{Y}^{-1}\boldsymbol{y}\right]\right\| e^{-||\boldsymbol{v}(\boldsymbol{n})||^2}\\
&= 2\pi||\boldsymbol{k}||\sum_{\Lambda\setminus S_R}\left\|\frac{1}{\sqrt{\pi}}\boldsymbol{T}^{-1}\boldsymbol{v}(\boldsymbol{n}) - \left[\left[\boldsymbol{Y}^{-1}\boldsymbol{y}\right]\right] - \left[\boldsymbol{Y}^{-1}\boldsymbol{y}\right]\right\| e^{-||\boldsymbol{v}(\boldsymbol{n})||^2}\\
&= 2\pi||\boldsymbol{k}||\sum_{\Lambda\setminus S_R}\left\|\frac{1}{\sqrt{\pi}}\boldsymbol{T}^{-1}\boldsymbol{v}(\boldsymbol{n}) - \boldsymbol{Y}^{-1}\boldsymbol{y}\right\| e^{-||\boldsymbol{v}(\boldsymbol{n})||^2}\\
&\leq 2\pi||\boldsymbol{k}||\sum_{\Lambda\setminus S_R}\left\|\frac{1}{\sqrt{\pi}}\boldsymbol{T}^{-1}\boldsymbol{v}(\boldsymbol{n})\right\| e^{-||\boldsymbol{v}(\boldsymbol{n})||^2} + 2\pi||\boldsymbol{k}||\left\|\boldsymbol{Y}^{-1}\boldsymbol{y}\right\|\sum_{\Lambda\setminus S_R} e^{-||\boldsymbol{v}(\boldsymbol{n})||^2}\\
&\leq 2\sqrt{\pi}||\boldsymbol{k}||\left\|\boldsymbol{T}^{-1}\right\|\sum_{\Lambda\setminus S_R}\|\boldsymbol{v}(\boldsymbol{n})\| e^{-||\boldsymbol{v}(\boldsymbol{n})||^2} + 2\pi||\boldsymbol{k}||\left\|\boldsymbol{Y}^{-1}\boldsymbol{y}\right\|\sum_{\Lambda\setminus S_R} e^{-||\boldsymbol{v}(\boldsymbol{n})||^2}, \qquad (27)
\end{aligned}$$

where the Cauchy-Schwarz and triangle inequalities were used. The second term in (27) is estimated as before. For the sum in the first term, Lemma 1 is used with $p = 1$. However, this only applied in the region where $||\boldsymbol{v}(\boldsymbol{n})||e^{-||\boldsymbol{v}(\boldsymbol{n})||^2}$ is subharmonic. According to Theorem 1, this holds when $R > \frac{1}{2}\sqrt{g+2+\sqrt{g^2+8}}$. Thus

$$\epsilon(R) \leq \sqrt{\pi} g\|\boldsymbol{k}\|\left(\frac{2}{\rho}\right)^g\left(\left\|\boldsymbol{T}^{-1}\right\|\Gamma\left(\frac{g+1}{2},(R-\rho/2)^2\right) + \sqrt{\pi}\left\|\boldsymbol{Y}^{-1}\boldsymbol{y}\right\|\Gamma\left(\frac{g}{2},(R-\rho/2)^2\right)\right), \quad (28)$$

provided $R > \frac{1}{2}\left(\sqrt{g+2+\sqrt{g^2+8}}+\rho\right)$.

Theorem 4 (Pointwise Approximation of the First Directional Derivative) *The directional derivative of the Riemann theta function along $\boldsymbol{k}$ is approximated by*

$$D(\boldsymbol{k})\,\theta(\boldsymbol{z}|\Omega) = e^{\pi \boldsymbol{y}\cdot\boldsymbol{Y}^{-1}\cdot\boldsymbol{y}} \times$$
$$\times 2\pi i\boldsymbol{k}\cdot\sum_{S_R}\left(\boldsymbol{n}-\left[\boldsymbol{Y}^{-1}\boldsymbol{y}\right]\right) e^{2\pi i\left(\frac{1}{2}\left(\boldsymbol{n}-\left[\boldsymbol{Y}^{-1}\boldsymbol{y}\right]\right)\cdot\boldsymbol{X}\cdot\left(\boldsymbol{n}-\left[\boldsymbol{Y}^{-1}\boldsymbol{y}\right]\right)+\left(\boldsymbol{n}-\left[\boldsymbol{Y}^{-1}\boldsymbol{y}\right]\right)\right)} e^{-||\boldsymbol{v}(\boldsymbol{n})||^2}, \quad (29)$$

with absolute error ϵ *on the scalar product of* $2\pi i\,\boldsymbol{k}$ *with the sum. Here* $S_R = \{\boldsymbol{v}(\boldsymbol{n}) \in \Lambda |\ ||\boldsymbol{v}(n)|| < R\}$, $\Lambda = \left\{\sqrt{\pi}\boldsymbol{T}(\boldsymbol{n} + [[\boldsymbol{Y}^{-1}\boldsymbol{y}]])\ |\boldsymbol{n} \in \mathbb{Z}^g\right\}$. *The shortest distance between any two points of* Λ *is denoted by* ρ. *Then the radius* R *is determined as the greater of* $\left(\sqrt{g+2+\sqrt{g^2+8}}+\rho\right)/2$ *and the real positive solution of* $\epsilon = \sqrt{\pi}g\|\boldsymbol{k}\|\left(\frac{2}{\rho}\right)^g\left(\left\|\boldsymbol{T}^{-1}\right\|\Gamma\left(\frac{g+1}{2},(R-\rho/2)^2\right)+\sqrt{\pi}\left\|\boldsymbol{Y}^{-1}\boldsymbol{y}\right\|\Gamma\left(\frac{g}{2},(R-\rho/2)^2\right)\right)$.

This theorem clearly gives a pointwise approximation: not only is the location of the ellipsoid S_R dependent on the evaluation point $\boldsymbol{z}$; more importantly its size R depends on it. This is the reason why this result cannot be extended to a uniform in $\boldsymbol{z}$ approximation theorem, as in the case of Theorem 3. By limiting the domain of $\boldsymbol{y}$, it is possible to obtain a uniform in $\boldsymbol{z}$ approximation theorem, valid over this domain:

Theorem 5 (Uniform Approximation of the First Directional Derivative) *The directional derivative of the Riemann theta function along* $\boldsymbol{k}$ *is approximated by*

$$D(\boldsymbol{k})\,\theta(\boldsymbol{z}|\Omega) = e^{\pi\boldsymbol{y}\cdot\boldsymbol{Y}^{-1}\cdot\boldsymbol{y}} \times \\ \times 2\pi i\boldsymbol{k}\cdot\sum_{U_R}\left(\boldsymbol{n}-\left[\boldsymbol{Y}^{-1}\boldsymbol{y}\right]\right)e^{2\pi i\left(\frac{1}{2}\left(\boldsymbol{n}-\left[\boldsymbol{Y}^{-1}\boldsymbol{y}\right]\right)\cdot\boldsymbol{X}\cdot\left(\boldsymbol{n}-\left[\boldsymbol{Y}^{-1}\boldsymbol{y}\right]\right)+\left(\boldsymbol{n}-\left[\boldsymbol{Y}^{-1}\boldsymbol{y}\right]\right)\right)}e^{-||\boldsymbol{v}(\boldsymbol{n})||^2}, \quad (30)$$

with absolute error ϵ *on the scalar product of* $2\pi i\,\boldsymbol{k}$ *with the sum, where the approximation is uniform in* $\boldsymbol{z}$, $\boldsymbol{z} = \boldsymbol{x} + i\boldsymbol{y}$, *for* $\boldsymbol{y} \in B_L^g(0)$. *Here* $\boldsymbol{v}(\boldsymbol{n}) = \sqrt{\pi}\boldsymbol{T}(\boldsymbol{n} + [[\boldsymbol{Y}^{-1}\boldsymbol{y}]])$, *and*

$$U_R = \left\{\boldsymbol{n} \in \mathbb{Z}^g | \pi(\boldsymbol{n}-\boldsymbol{c})\cdot\boldsymbol{Y}\cdot(\boldsymbol{n}-\boldsymbol{c}) < R^2, |c_j| < 1/2, j = 1,\ldots,g\right\}. \quad (31)$$

Let $\Lambda = \left\{\sqrt{\pi}\boldsymbol{T}(\boldsymbol{n} + [[\boldsymbol{Y}^{-1}\boldsymbol{y}]])\ |\boldsymbol{n} \in \mathbb{Z}^g\right\}$. *The shortest distance between any two points of* Λ *is denoted by* ρ. *Then the radius* R *is determined as the greater of* $\left(\sqrt{g+2+\sqrt{g^2+8}}+\rho\right)/2$ *and the real positive solution of* $\epsilon = \sqrt{\pi}g\|\boldsymbol{k}\|\left\|\boldsymbol{T}^{-1}\right\|\left(\frac{2}{\rho}\right)^g\left(\Gamma\left(\frac{g+1}{2},(R-\rho/2)^2\right)+\sqrt{\pi}L\left\|\boldsymbol{T}^{-1}\right\|\Gamma\left(\frac{g}{2},(R-\rho/2)^2\right)\right)$.

Proof. This follows easily from the Pointwise Approximation result, by using $\|\boldsymbol{Y}^{-1}\boldsymbol{y}\| \le \|\boldsymbol{Y}^{-1}\|\|\boldsymbol{y}\|$ and $\|\boldsymbol{Y}^{-1}\| \le \|\boldsymbol{T}^{-1}\|^2$. ■

This theorem is not as useful as Theorem 3, due to the restriction on the size of $\|\boldsymbol{y}\|$. When it is used, it results in a situation where many terms are included which are only relevant for the evaluation of values of the directional derivative near $\|\boldsymbol{y}\| = L$. However, for graphing or other purposes where many evaluations of $D(\boldsymbol{k})\theta(\boldsymbol{z}|\boldsymbol{\Omega})$ are required, centered around an area for z where $\boldsymbol{y} = 0$, such a uniform approximation is usually beneficial compared to the pointwise approximation. It was used in Fig. 5a to illustrate the linear growth of the derivative of the Riemann theta function parametrized by (22), after removal of the exponential growth.

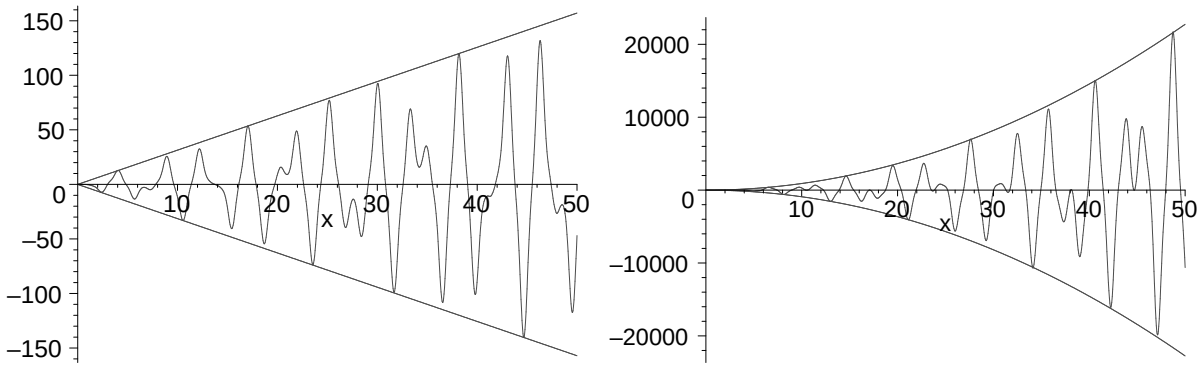

(a) (b)

Figure 5: Two directional derivatives of the Riemann theta function $\theta(0, ix|\Omega)$ with Ω as in (22). As before, the exponential growth-factor has been factored out. In (a) the directional derivative of order one with $\boldsymbol{k} = (1, 0)$ is shown. Fig. (b) illustrates the quadratic growth of the directional derivative of order two, with $\boldsymbol{k}^{(1)} = \boldsymbol{k}^{(2)} = (1, 0)$.

6.2 Second-order derivatives

With $N = 2$, (5) gives

$$\begin{aligned}
& e^{-\pi \boldsymbol{y}\cdot\boldsymbol{Y}^{-1}\cdot\boldsymbol{y}}\, D(\boldsymbol{k}^{(1)}, \boldsymbol{k}^{(2)})\theta(\boldsymbol{z}|\boldsymbol{\Omega}) \\
= \;& (2\pi i)^2 \sum_{\boldsymbol{n}\in\mathbb{Z}^g} \Big(\boldsymbol{k}^{(1)} \cdot \big(\boldsymbol{n} - \big[\boldsymbol{Y}^{-1}\boldsymbol{y}\big]\big)\Big)\Big(\boldsymbol{k}^{(2)} \cdot \big(\boldsymbol{n} - \big[\boldsymbol{Y}^{-1}\boldsymbol{y}\big]\big)\Big) \times \\
& \qquad \times e^{2\pi i\left(\frac{1}{2}\left(\boldsymbol{n}-\left[\boldsymbol{Y}^{-1}\boldsymbol{y}\right]\right)\cdot\boldsymbol{X}\cdot\left(\boldsymbol{n}-\left[\boldsymbol{Y}^{-1}\boldsymbol{y}\right]\right)+\left(\boldsymbol{n}-\left[\boldsymbol{Y}^{-1}\boldsymbol{y}\right]\right)\right)} e^{-||\boldsymbol{v}(\boldsymbol{n})||^2} \\
= \;& (2\pi i)^2 \lim_{R\to\infty} \sum_{S_R} \Big(\boldsymbol{k}^{(1)} \cdot \big(\boldsymbol{n} - \big[\boldsymbol{Y}^{-1}\boldsymbol{y}\big]\big)\Big)\Big(\boldsymbol{k}^{(2)} \cdot \big(\boldsymbol{n} - \big[\boldsymbol{Y}^{-1}\boldsymbol{y}\big]\big)\Big) \times \\
& \qquad \times e^{2\pi i\left(\frac{1}{2}\left(\boldsymbol{n}-\left[\boldsymbol{Y}^{-1}\boldsymbol{y}\right]\right)\cdot\boldsymbol{X}\cdot\left(\boldsymbol{n}-\left[\boldsymbol{Y}^{-1}\boldsymbol{y}\right]\right)+\left(\boldsymbol{n}-\left[\boldsymbol{Y}^{-1}\boldsymbol{y}\right]\right)\right)} e^{-||\boldsymbol{v}(\boldsymbol{n})||^2}
\end{aligned} \tag{32}$$

where S_R and $\boldsymbol{v}(\boldsymbol{n})$ are defined as in (8). Using similar steps as before, and using Lemmas 1 and 2 with $p = 2$ results in the following theorems:

Theorem 6 (Pointwise Approximation of the Second Directional Derivative) *The directional derivative of second order along $\boldsymbol{k}^{(1)}$ and $\boldsymbol{k}^{(2)}$ of the Riemann theta function is approximated by*

$$\begin{aligned}
D(\boldsymbol{k}^{(1)}, \boldsymbol{k}^{(2)})\,\theta(\boldsymbol{z}|\boldsymbol{\Omega}) = e^{\pi \boldsymbol{y}\cdot\boldsymbol{Y}^{-1}\cdot\boldsymbol{y}} \times \\
\times (2\pi i)^2 \sum_{S_R} \Big(\boldsymbol{k}^{(1)} \cdot \big(\boldsymbol{n} - \big[\boldsymbol{Y}^{-1}\boldsymbol{y}\big]\big)\Big)\Big(\boldsymbol{k}^{(2)} \cdot \big(\boldsymbol{n} - \big[\boldsymbol{Y}^{-1}\boldsymbol{y}\big]\big)\Big) \times \\
\times e^{2\pi i\left(\frac{1}{2}\left(\boldsymbol{n}-\left[\boldsymbol{Y}^{-1}\boldsymbol{y}\right]\right)\cdot\boldsymbol{X}\cdot\left(\boldsymbol{n}-\left[\boldsymbol{Y}^{-1}\boldsymbol{y}\right]\right)+\left(\boldsymbol{n}-\left[\boldsymbol{Y}^{-1}\boldsymbol{y}\right]\right)\right)} e^{-||\boldsymbol{v}(\boldsymbol{n})||^2}
\end{aligned} \tag{33}$$

with absolute error ϵ on the product of $(2\pi i)^2$ with the sum. Here $S_R = \{\boldsymbol{v}(\boldsymbol{n}) \in \Lambda |\ ||\boldsymbol{v}(n)|| < R\}$, $\Lambda = \left\{\sqrt{\pi}\boldsymbol{T}(\boldsymbol{n} + [[\boldsymbol{Y}^{-1}\boldsymbol{y}]])\ |\boldsymbol{n} \in \mathbb{Z}^g\right\}$. The shortest distance between any two points of Λ is denoted by ρ. Then the radius R is determined as the greater of $\left(\sqrt{g+4+\sqrt{g^2+16}}+\rho\right)/2$ and the real positive solution of $\epsilon = 2\pi g \|\boldsymbol{k}^{(1)}\| \|\boldsymbol{k}^{(2)}\| \left(\frac{2}{\rho}\right)^g \left(\left\|\boldsymbol{T}^{-1}\right\|^2 \Gamma\left(\frac{g+2}{2}, (R-\rho/2)^2\right) + 2\sqrt{\pi}\left\|\boldsymbol{T}^{-1}\right\| \left\|\boldsymbol{Y}^{-1}\boldsymbol{y}\right\| \Gamma\left(\frac{g+1}{2}, (R-\rho/2)^2\right) + \pi \left\|\boldsymbol{Y}^{-1}\boldsymbol{y}\right\|^2 \Gamma\left(\frac{g}{2}, (R-\rho/2)^2\right)\right)$.

Theorem 7 (Uniform Approximation of the Second Directional Derivative) *The directional derivative of second order along $\boldsymbol{k}^{(1)}$ and $\boldsymbol{k}^{(2)}$ of the Riemann theta function is approximated by*

$$\begin{aligned} D(\boldsymbol{k}^{(1)}, \boldsymbol{k}^{(2)})\, \theta(\boldsymbol{z}|\boldsymbol{\Omega}) = e^{\pi \boldsymbol{y}\cdot\boldsymbol{Y}^{-1}\cdot\boldsymbol{y}} \times \\ \times (2\pi i)^2 \sum_{U_R} \left(\boldsymbol{k}^{(1)} \cdot \left(\boldsymbol{n} - \left[\boldsymbol{Y}^{-1}\boldsymbol{y}\right]\right)\right) \left(\boldsymbol{k}^{(2)} \cdot \left(\boldsymbol{n} - \left[\boldsymbol{Y}^{-1}\boldsymbol{y}\right]\right)\right) \times \\ \times e^{2\pi i \left(\frac{1}{2}\left(\boldsymbol{n} - \left[\boldsymbol{Y}^{-1}\boldsymbol{y}\right]\right)\cdot\boldsymbol{X}\cdot\left(\boldsymbol{n} - \left[\boldsymbol{Y}^{-1}\boldsymbol{y}\right]\right) + \left(\boldsymbol{n} - \left[\boldsymbol{Y}^{-1}\boldsymbol{y}\right]\right)\right)} e^{-||\boldsymbol{v}(\boldsymbol{n})||^2} \end{aligned} \tag{34}$$

with absolute error ϵ on the scalar product of $(2\pi i)^2$ with the sum, where the approximation is uniform in $\boldsymbol{z}$, $\boldsymbol{z} = \boldsymbol{x} + i\boldsymbol{y}$, for $\boldsymbol{y} \in B_L^g(0)$. Here $\boldsymbol{v}(\boldsymbol{n}) = \sqrt{\pi}\boldsymbol{T}(\boldsymbol{n} + [[\boldsymbol{Y}^{-1}\boldsymbol{y}]])$, and

$$U_R = \left\{\boldsymbol{n} \in \mathbb{Z}^g | \pi(\boldsymbol{n} - \boldsymbol{c}) \cdot \boldsymbol{Y} \cdot (\boldsymbol{n} - \boldsymbol{c}) < R^2, |c_j| < 1/2, j = 1, \ldots, g\right\}. \tag{35}$$

Let $\Lambda = \left\{\sqrt{\pi}\boldsymbol{T}(\boldsymbol{n} + [[\boldsymbol{Y}^{-1}\boldsymbol{y}]])\ |\boldsymbol{n} \in \mathbb{Z}^g\right\}$. The shortest distance between any two points of Λ is denoted by ρ. Then the radius R is determined as the greater of $\left(\sqrt{g+4+\sqrt{g^2+16}}+\rho\right)/2$ and the real positive solution of $\epsilon = 2\pi g \|\boldsymbol{k}^{(1)}\| \|\boldsymbol{k}^{(2)}\| \left(\frac{2}{\rho}\right)^g \left\|\boldsymbol{T}^{-1}\right\|^2 \left(\Gamma\left(\frac{g+2}{2}, (R-\rho/2)^2\right) + 2\sqrt{\pi}\left\|\boldsymbol{T}^{-1}\right\| L\Gamma\left(\frac{g+1}{2}, (R-\rho/2)^2\right) + \pi L^2 \left\|\boldsymbol{T}^{-1}\right\|^2 \Gamma\left(\frac{g}{2}, (R-\rho/2)^2\right)\right)$.

The same remarks as for the first-order directional derivative are valid here as well. The last theorem has limited use due to its restriction on the size of $\|\boldsymbol{y}\|$. It was used in Fig. 5b to illustrate the quadratic growth of the derivative of the Riemann theta function parametrized by (22), after removal of the exponential growth.

7 Siegel transformations

Consider the Riemann theta function parametrized by the Riemann matrix

$$\boldsymbol{\Omega} = \frac{-1}{2\pi i} \begin{pmatrix} 111.207 & 96.616 \\ 96.616 & 83.943 \end{pmatrix}. \tag{36}$$

This is the example from Appendix C of [8], adapted to the definition of the theta function used here. It was used in [8] to illustrate the need for a fundamental region of Riemann matrices. The problem arising is that the ellipsoid (ellipse, in this case) determining the summation indices in the approximation of the oscillatory part of the Riemann theta function is very eccentric. The

eigenvalues of $\boldsymbol{Y}$ are 31.0587 and 0.000324, resulting in an eccentricity of the ellipse of $1-0.54\ 10^{-10}$. Thus very few of the summation indices closest to $(0,0)$ play a part in the evaluation of the Riemann theta function. This was the problem addressed in [8]. Since our algorithm incorporates a way to determine which summation indices lie inside the ellipsoid determined by $\boldsymbol{Y}$, this is not troublesome here. What is troublesome is that the ellipsoid contains many integer points: already for $\epsilon = 0.001$, the evaluation of $\theta(0,0|\boldsymbol{\Omega})$ requires the inclusion of 109 terms. This is largely due to the fact that the ellipsoid lies along a rational direction in the (n_1, n_2) plane, as illustrated in Fig. 6.

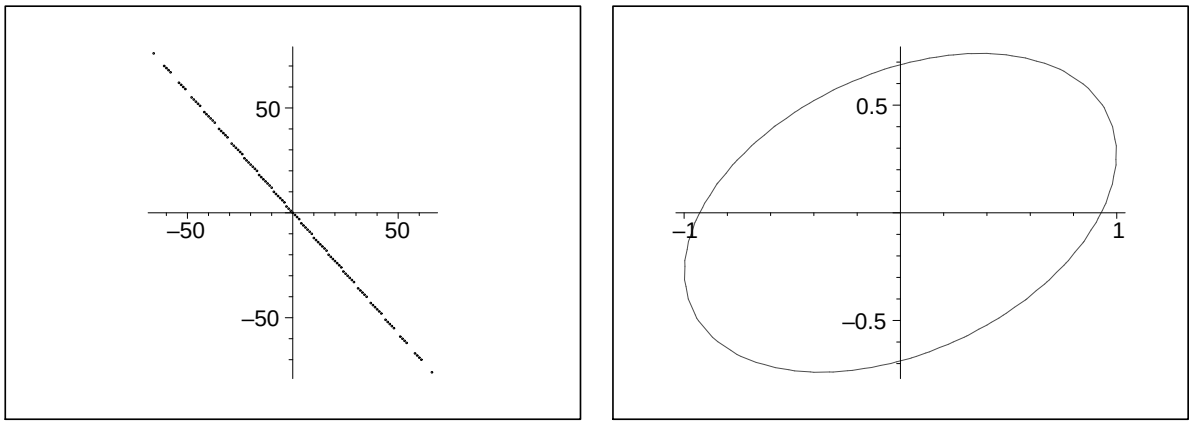

(a) (b)

Figure 6: The summation indices for the evaluation of the oscillatory part of $\theta(0,0|\boldsymbol{\Omega})$ and $\theta(0,0|\hat{\boldsymbol{\Omega}})$ with $\epsilon = 0.001$. In Fig. (a), with $\boldsymbol{\Omega}$, there are 109 summation indices, all inside a very eccentric ellipse lying along the line $n_2 = -n_1$. Figure (b) corresponds to $\hat{\boldsymbol{\Omega}}$, which was obtained from $\boldsymbol{\Omega}$ by way of a modular transformation (37). Now only one summation index lies inside the ellipse: $(n_1, n_2) = (0,0)$.

In such cases, the transformation properties of the Riemann theta function can be used to great advantage. Just as the elliptic functions and the Jacobian theta functions, the Riemann theta function has a modular transformation property. The modular transformation is a transformation on the Riemann matrix. The transformed Riemann matrix defines a Riemann theta function, just as the original Riemann matrix does. These two Riemann theta functions are related: up to an affine transformation of the argument $\boldsymbol{z}$ and an overall scaling factor, they are identical. For details, see [14].

Remarks

- Geometrically, the modular transformation on the Riemann matrix is a transformation on the period lattice of the Riemann theta function. Thus the modular transformation property relates two Riemann theta functions with different period lattices [14].
- For Riemann matrices originating from Riemann surfaces, the modular transformation amounts to choosing a different canonical intersection basis for the homology of the Riemann surface [7]. Then it is not a surprise that the solutions of differential equations written in terms of

Abelian functions do not depend on this choice. One could think of this as a discrete symmetry of the solutions of the differential equation. Thus for such applications it is unimportant to transform the Riemann theta function, as long as one consistently does all calculations with a preferred homology basis.

Let

$$\Gamma = \begin{pmatrix} \boldsymbol{a} & \boldsymbol{b} \\ \boldsymbol{c} & \boldsymbol{d} \end{pmatrix}$$

be a symplectic matrix with integer elements, $\Gamma \in SP(2g, \mathbb{Z})$, *i.e.*,

$$\begin{pmatrix} \boldsymbol{a} & \boldsymbol{b} \\ \boldsymbol{c} & \boldsymbol{d} \end{pmatrix} \begin{pmatrix} \boldsymbol{0}_g & \boldsymbol{I}_g \\ -\boldsymbol{I}_g & \boldsymbol{0}_g \end{pmatrix} \begin{pmatrix} \boldsymbol{a}^T & \boldsymbol{c}^T \\ \boldsymbol{b}^T & \boldsymbol{d}^T \end{pmatrix} = \begin{pmatrix} \boldsymbol{0}_g & \boldsymbol{I}_g \\ -\boldsymbol{I}_g & \boldsymbol{0}_g \end{pmatrix},$$

where $\boldsymbol{a}$, $\boldsymbol{b}$, $\boldsymbol{c}$, and $\boldsymbol{d}$ are $g \times g$ matrices with integer elements, $\boldsymbol{I}_g$ and $\boldsymbol{0}_g$ are the $g \times g$ identity and nul matrix, respectively. $SP(2g, \mathbb{Z})$ is called the modular group. An element of the modular group transforms the Riemann matrix $\boldsymbol{\Omega}$ according to

$$\boldsymbol{\Omega} \to \hat{\boldsymbol{\Omega}} = (\boldsymbol{a}\boldsymbol{\Omega} + \boldsymbol{b})(\boldsymbol{c}\boldsymbol{\Omega} + \boldsymbol{d})^{-1}. \tag{37}$$

The modular group is generated by the three generators Γ_1, Γ_2 and Γ_3 [14]:

$$\Gamma_1 = \begin{pmatrix} \boldsymbol{a} & \boldsymbol{0}_g \\ \boldsymbol{0}_g & (\boldsymbol{a}^{-1})^T \end{pmatrix}, \ \hat{\boldsymbol{\Omega}} = \boldsymbol{a}\boldsymbol{\Omega}\boldsymbol{a}^{-1}, \ \theta(\boldsymbol{A}\boldsymbol{z}|\boldsymbol{A}\boldsymbol{\Omega}\boldsymbol{A}^T) = \theta(\boldsymbol{z}|\boldsymbol{\Omega}), \tag{38}$$

$$\Gamma_2 = \begin{pmatrix} \boldsymbol{1}_g & \boldsymbol{b} \\ \boldsymbol{0}_g & \boldsymbol{1}_g \end{pmatrix}, \quad \hat{\boldsymbol{\Omega}} = \boldsymbol{\Omega} + \boldsymbol{b}, \quad \theta(\boldsymbol{z}|\boldsymbol{\Omega} + \boldsymbol{b}) = \theta(\boldsymbol{z} + \mathrm{diag}(\boldsymbol{b})/2|\boldsymbol{\Omega}), \tag{39}$$

$$\Gamma_3 = \begin{pmatrix} \boldsymbol{0}_g & -\boldsymbol{1}_g \\ \boldsymbol{1}_g & \boldsymbol{0}_g \end{pmatrix}, \quad \hat{\boldsymbol{\Omega}} = -\boldsymbol{\Omega}^{-1}, \quad \theta(\boldsymbol{\Omega}^{-1}\boldsymbol{z}| - \boldsymbol{\Omega}^{-1}) = \sqrt{\det(-i\boldsymbol{\Omega})}\, e^{\pi i \boldsymbol{z}\cdot\boldsymbol{\Omega}^{-1}\cdot\boldsymbol{z}} \theta(\boldsymbol{z}|\boldsymbol{\Omega}), \tag{40}$$

where $\mathrm{diag}(\boldsymbol{b})$ denotes the diagonal part of the matrix $\boldsymbol{b}$, which has even diagonal elements, and $\boldsymbol{b}^T = \boldsymbol{b}$. In the last equation, the branch of the square root is used which is positive when its argument is positive.

Since any modular transformation is a composition of these three types, the transformation formulas on the Riemann theta function on the right can be used to calculate the effect of the resulting modular transformation on the Riemann theta function.

From our point of view, the goal is to find a transformation on the Riemann matrix (*i.e.*, a composition of generating modular transformations) to minimize the eccentricity of the ellipsoid determined by the transformed matrix. The algorithm described in this section is due to Siegel [18]. Siegel's goal was to construct a fundamental region for Riemann matrices, analogous to the elliptic case. The algorithm iteratively finds a new Riemann matrix with improved (*i.e.*, smaller) eccentricity for the ellipsoid it determines. However, the algorithm is not optimal. An optimal algorithm does not appear to be known. The description below is an algorithmic description of Siegel's [18], aimed at implementation. This implementation is included in Maple 8.

Theorem 8 (Siegel Reduction) *Every Riemann matrix $\boldsymbol{\Omega}$ can, by means of a modular transformation (37), be reduced to a Riemann matrix $\hat{\boldsymbol{\Omega}} = \hat{\boldsymbol{X}} + i\hat{\boldsymbol{Y}}, \hat{\boldsymbol{Y}} = \boldsymbol{T}^T\boldsymbol{T}$, with $\hat{\boldsymbol{X}}$ ($\hat{\boldsymbol{Y}}$) the real (imaginary) part of $\hat{\boldsymbol{\Omega}}$, and $\boldsymbol{T}$ upper triangular, such that*

1. $|\hat{X}_{jk}| \leq 1/2, \quad j,k = 1 \ldots g,$
2. *the length of the shortest lattice vector ρ of the lattice generated by the columns of $\boldsymbol{T}$ is bound from below by $\sqrt{\sqrt{3}/2}$, and*
3. *$max\{|N_j| : \|\boldsymbol{TN}\| \leq R, R > 0, fixed, \boldsymbol{N} \in \mathbb{Z}^g\}$ has an upper bound which only depends on g and R. Thus this upper bound is independent of $\boldsymbol{T}$.*

The second condition eliminates ellipsoids with high eccentricity. The theorem in effect guarantees an upper bound for the number of summation indices required for the evaluation of the oscillatory part of a genus g Riemann theta function with a prescribed error ϵ (and thus R). This upper bound does not depend on the reduced Riemann matrix $\hat{\boldsymbol{\Omega}}$.

Proof:

- **Proof of statement 1:** Using (39),

$$\boldsymbol{\Omega} \to \boldsymbol{\Omega} - [\mathrm{Re}(\boldsymbol{\Omega})]. \tag{41}$$

- **Proof of statement 2:** We can assume that $\boldsymbol{T}$ is lattice reduced, using the LLL algorithm [13]. Then $\rho = T_{11} = \sqrt{\hat{Y}_{11}}$, since $\boldsymbol{T}$ is upper triangular. Siegel [18] shows that the determinants of the imaginary parts of two Riemann matrices connected by a modular transformation (37) are related by

$$|\det(\hat{\boldsymbol{Y}})| = \frac{|\det(\boldsymbol{Y})|}{|\det(\boldsymbol{c\Omega} + \boldsymbol{d})|^2}, \tag{42}$$

  where $\boldsymbol{Y}$, $\hat{\boldsymbol{Y}}$ are the imaginary parts of $\boldsymbol{\Omega}$ and $\hat{\boldsymbol{\Omega}}$, respectively. Using the modular transformation with

$$\boldsymbol{a} = \begin{pmatrix} 0 & \boldsymbol{0}^T \\ \boldsymbol{0} & \boldsymbol{1}_{g-1} \end{pmatrix}, \boldsymbol{b} = \begin{pmatrix} -1 & \boldsymbol{0}^T \\ \boldsymbol{0} & \boldsymbol{0}_{g-1} \end{pmatrix}, \boldsymbol{c} = \begin{pmatrix} 1 & \boldsymbol{0}^T \\ \boldsymbol{0} & \boldsymbol{0}_{g-1} \end{pmatrix}, \boldsymbol{d} = \begin{pmatrix} 0 & \boldsymbol{0}^T \\ \boldsymbol{0} & \boldsymbol{1}_{g-1} \end{pmatrix},$$

  with $\boldsymbol{0}$ the $(g-1)$-dimensional zero vector, (42) becomes

$$|\det(\hat{\boldsymbol{Y}})| = \frac{|\det(\boldsymbol{Y})|}{|\Omega_{11}|^2}.$$

  If $|\Omega_{11}| < 1$, this transformation is applied. This transformation preceeded by the transformation giving (41) is repeated until $|\hat{\Omega}_{11}| \geq 1$. Then $|\hat{\Omega}_{11}|^2 = \hat{X}_{11}^2 + \hat{Y_{11}}^2 \geq 1$. Thus $\rho = \sqrt{\hat{Y}_{11}} \geq \sqrt{\sqrt{1 - \hat{X}_{11}^2}} \geq \sqrt{\sqrt{3}/2}$, since $\hat{X}_{11}^2 \leq 1/4$. It remains to be shown that this iteration terminates. This is demonstrated by Siegel [18].

- **Proof of statement 3:** If $\boldsymbol{T}$ is lattice reduced using the LLL algorithm, then (see [13])
  - $T_{jj} > 0, \qquad 1 \leq j \leq g,$
  - $|T_{jk}| \leq |T_{jj}|/2, \qquad 1 \leq j < k \leq g,$

$*$ $T_{j,j+1}^2 + T_{j+1,j+1}^2 \geq T_{jj}^2, \quad 1 \leq j < g.$

It follows from these last two properties that $T_{jj} \geq \frac{\sqrt{3}}{2} T_{j-1,j-1}$, for $j \in (1, g]$, and thus $T_{jj} \geq \left(\frac{\sqrt{3}}{2}\right)^{j-1} \rho$. Then $\max\{|N_j| : \|\boldsymbol{TN}\| \leq R, R > 0, \text{fixed}, \boldsymbol{N} \in \mathbb{Z}^g\} \leq \max\{|N_j| : |(\boldsymbol{TN})_j| \leq R, R > 0, \text{fixed}, j \in [1, g], \boldsymbol{N} \in \mathbb{Z}^g\} \leq R/r$. ■

Note that the preceding proof indeed shows that the new ellipsoid defined by $\|\boldsymbol{TN}\| = R$ has an eccentricity bound away from 1.

This algorithm was used on the Riemann matrix given in (36), with great success: after applying the algorithm, the evaluation of the oscillatory part of the Riemann theta function parametrized by the transformed Riemann matrix at $\boldsymbol{z} = (0, 0)$ with absolute error $\epsilon = 0.001$ requires only one summation index: $(n_1, n_2) = (0, 0)$. The modular transformation used is

$$\Gamma = \begin{pmatrix} 0 & 0 & 8 & 7 \\ 0 & 0 & 7 & 6 \\ 6 & -7 & 0 & 0 \\ -7 & 8 & 0 & 0 \end{pmatrix},$$

resulting in

$$\hat{\boldsymbol{\Omega}} = \begin{pmatrix} 7.94597 & -3.94937 \\ -3.94937 & 14.4545 \end{pmatrix},$$

giving an ellipsoid with eccentricity 0.927921, with a major-axes ratio $\approx 3/8$.

Acknowledgements

The research presented in this paper was supported through NSF grants DMS-9805983, DMS-0071568 (BD), SFB288 (Differential geometry and quantum physics, AB, MH, MS) and DMS-0098034 (MvH).

Appendix A: The Maple implementation

The maple code can be viewed by typing the following commands in Maple 8 or later:

```
interface(verboseproc=2);
op(RiemannTheta);
op(‘RiemannTheta/doit‘);
op(‘RiemannTheta/boundingellipsoid‘);
op(‘RiemannTheta/findvectors‘);
op(‘RiemannTheta/make_proc‘);
op(‘RiemannTheta/finitesum‘);
```

It can also be downloaded from `http://www.math.fsu.edu/ hoeij/RiemannTheta/`.

The procedure `RiemannTheta` uses a variety of arguments. The first two of these are required. All others are optional and can be omitted.

1. A $g \times g$ Riemann matrix $\mathbf{\Omega}$.

2. A g-dimensional vector $\boldsymbol{z}$.

3. A number ϵ indicating the desired accuracy of the result.

4. A (possibly empty) list of vectors. Each vector is used as in (4) for the calculation of directional derivatives.

5. Other optional arguments: The algorithm computes the exponential growth factor a and the oscillatory part b separately. The user can specify if a and b should both be given in the output, or if the output should consist of only $\exp(a)b$.

`RiemannTheta` distinguishes two cases:

a. z evaluates to an element of $\mathbb{C}^g$.

b. z does not evaluate to an element of $\mathbb{C}^g$, because it contains one or more variables that have no assigned values.

If no directional derivatives are given, then `RiemannTheta` computes either a list of two complex numbers $[a, b]$ or one complex number $e^a b$ such that $\theta(\Omega, z) \approx e^a b$. Here b is bounded for $z \in \mathbb{C}^g$, and has error less than ϵ. If directional derivatives are given, then b grows polynomially. For case b, it is not guaranteed that b's error is bounded by ϵ unless an a-priori bound for z is known.

If `RiemannTheta` is called, then the set S of points in the "ellipsoid" described in Figure 3 is calculated. See Figure 3(a) for case a, and Figure 3(b) for case b. Following the computation, `RiemannTheta` returns an expression that contains `'RiemannTheta/finitesum'(args)`. Here `'RiemannTheta/finitesum'` is a procedure and `args` is a list of arguments. These arguments contain all information necessary to compute the value of RiemannTheta with the specified accuracy. This information includes $\boldsymbol{z}$, $\mathbf{\Omega}$ and S, but reorganized into a form more convenient for summation (*e.g.*, the real and imaginary parts of the input are separated, as are the integer and non-integer part before summation over the set S is begun). However, the summation is not done unless $\boldsymbol{z} \in \mathbb{C}^g$. Only if $\boldsymbol{z}$ contains no unassigned variables can $\boldsymbol{z}$ be evaluated to an element of $\mathbb{C}^g$, and only in this case will `'RiemannTheta/finitesum'(args)` return a number. This number then becomes the output of `RiemannTheta`. If $\boldsymbol{z}$ does contain unassigned variables, then the summation will be delayed, and `'RiemannTheta/finitesum'(args)` will remain unevaluated. Thus, using variables in $\boldsymbol{z}$ instead of complex numbers causes `RiemannTheta` to return an answer that contains an unevaluated procedure. This is useful if one wants to calculate more than one value of `RiemannTheta` for the same $\mathbf{\Omega}$. If only a single value of `RiemannTheta` is wanted, one gives `RiemannTheta` a vector $\boldsymbol{z} \in \mathbb{C}^g$. If one wants to compute `RiemannTheta` for many $\boldsymbol{z}$'s (*e.g.*, for plotting purposes) then one includes variables in $\boldsymbol{z}$. The procedure which is the output of `RiemannTheta` is then used for evaluation. This way the set of points in Figure 3(b) is computed only once, which is more efficient than computing the points in Figure 3(a) for each value of $\boldsymbol{z}$.

Below is a verbatim example of interactive use of Maple and `RiemannTheta`.

```
> r3 := sqrt(-3)/3:
> M := evalf( Matrix(2,2,[[1+2*r3,-1-r3],[-1-r3,1+2*r3]]) );
                    [ 1. + 1.154700539 I     -1. - 0.5773502693 I]
               M := [                                             ]
                    [-1. - 0.5773502693 I     1. + 1.154700539 I ]
> eps := 0.001:
> z := [1-I,  I+1]; # Here z contains no variables.
                               z := [1 - I, 1 + I]
> R := RiemannTheta(z, M, [], eps);
                                                          -8
                     R := -21.76547256 - 0.2323298326 10   I
> L := RiemannTheta(z, M, [], eps, output=list);
                                                                -10
           L := [3.627598727, -0.5785248137 - 0.6175311504 10    I]
> a := L[1]:
> b := L[2]:
> R := exp(a)*b;
                                                          -8
                     R := -21.76547256 - 0.2323298326 10   I
> z := [X,    I+1];   # Now z contains 1 variable.
                                 z := [X, 1 + I]
> R := RiemannTheta(z, M, [], eps, output=list);
                         2
R := [3.627598726 Im(X)  + 3.627598724 Im(X) + 3.627598726,
     RiemannTheta/finitesum( ... ) ]
> eval(R, X=1-I);
                                                           -10
              [3.627598728, -0.57852736323 - 0.61753198638 10    I]
> eval(R, X=1-2*I);
                                                            -9
               [10.88279618, 0.62464131574 - 0.56009279234 10   I]
> eval(R, X=1-3*I);
                                                          -10
              [25.39319109, 0.44006321314 - 0.92901122197 10    I]
```

Appendix B: The Java implementation

The Java implementation is an adaptation of an earlier implementation in C which has been in use since 1994. The Java version uses the definition (1) of the Riemann theta function. The C version employed a different definition:

$$\tilde{\theta}\left(\boldsymbol{z}|\boldsymbol{\Omega}\right)=\sum_{\boldsymbol{n}\in\mathbb{Z}^g}e^{\frac{1}{2}\boldsymbol{n}\cdot\boldsymbol{B}\cdot\boldsymbol{n}+\boldsymbol{z}\cdot\boldsymbol{n}}=\theta\left(\frac{\boldsymbol{z}}{2\pi i}\Big|\frac{\boldsymbol{B}}{2\pi i}\right),$$

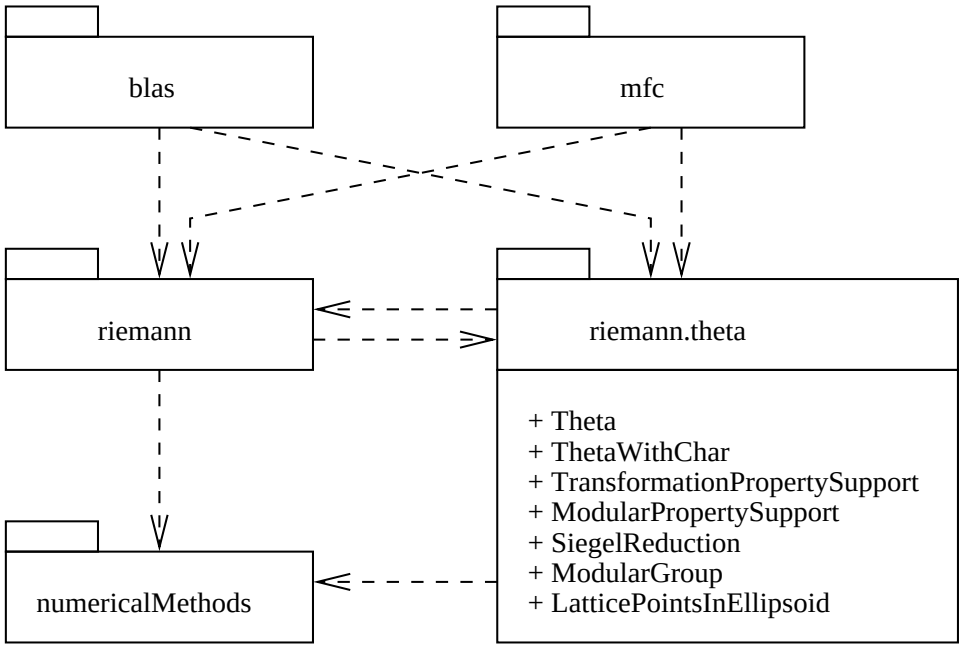

Figure 7: Dependencies of the package `riemann.theta`.

where the real part of $\boldsymbol{B}$ is negative definite.

The java implementation of the Riemann theta function is realized in the package `riemann.theta`, which includes the public classes `LatticePointsInEllipsoid`, `ModularGroup`, `SiegelReduction`, `ModularPropertySupport`, `TransformationPropertySupport`, `Theta` and `ThetaWithChar`. Unlike other programming languages, Java does not incorporate a complex type, thus the package requires an implementation of such, realized in `mfc.number.Complex`. The implementation also requires the packages `blas` (basic linear algebra system), and `numericalMethods`. This last package is used only in internal computations. Figure 7 illustrates these dependencies, showing only the classes within `riemann.theta`.

The class `Theta` implements the uniform approximation theorems 3, 5 and 7. The default error used by the program is the FFE, with default error tolerance set to 10^{-7}. Siegel's reduction algorithm as described in section 7 is always used.

Example: Consider the slices of a genus 2 Riemann theta function shown in Figure 4. The complete Java program for computing the data in one of these slices is:

```
import riemann.theta.Theta;
import mfc.number.Complex;
import blas.ComplexVector;
import blas.ComplexMatrix;
public class ExampleSlice {
public static void main( String [] argv ) {
  // create the period matrix
```

```
    ComplexMatrix B = new ComplexMatrix( 2 );
    // set the period matrix
    B.set( 0,0, 1.690983006, 0.9510565162 );
    B.set( 0,1, 1.500000000, 0.3632712640 );
    B.set( 1,0, 1.500000000, 0.3632712640 );
    B.set( 1,1, 1.309016994, 0.9510565162 );
    // use the different normalization
    B.setTimes( new Complex( 0, 2 * Math.PI ) );
    // create a complex argument vector
    ComplexVector V = new ComplexVector( 2 );
    // create a theta function instance with period matrix
    Theta theta = new Theta( B );
    // create storage for the slice
    Complex[][] slice = new Complex[101][101];
    // loop over grid
    for( int i=0; i<101; i++ )
      for( int j=0; j<101; j++ ) {
        // set grid vector
        V.set( 1, 2 * i *Math.PI / 100, 2 * j * Math.PI / 100 );
        // evaluate theta function at grid vector
        slice[i][j] = theta.theta( V );
      }
    }
}
```

To compile this example, the user needs the Java archives `riemann.jar`, `blas.jar`, `mfc.jar` and `numericalMethods.jar` in their classpath. These archives, as well as their source code and documentation is available from `www-sfb288.math.tu-berlin.de/ jem`.

The package `riemann.theta` also includes a class `ThetaWithChar` which incorporates Riemann theta functions with characteristics.

References

[1] *Handbook of mathematical functions, with formulas, graphs and mathematical tables*. National Bureau of Standards, Washington, D.C., 1966. Edited by M. Abramowitz and I. A. Stengun.

[2] A. I. Babich and A. I. Bobenko. Willmore tori with umbilic lines and minimal surfaces in hyperbolic space. *Duke Math. J.*, 72(1):151–185, 1993.

[3] E. D. Belokolos, A. I. Bobenko, V. Z. Enol'skii, A. R. Its, and V. B. Matveev. *Algebro-geometric approach to nonlinear integrable problems*. Springer Series in Nonlinear Dynamics. Springer-Verlag, Berlin, 1994.

[4] A. I. Bobenko. All constant mean curvature tori in r^3, s^3, h^3 in terms of theta-functions. *Math. Ann.*, 290:209–245, 1991.

[5] A. I. Bobenko and L. A. Bordag. Periodic multiphase solutions of the kadomsev-petviashvili equation. *J. Phys. A.*, 22:1259–1274, 1989.

[6] B. Deconinck and M. van Hoeij. Computing Riemann matrices of algebraic curves. *Physica D*, 152–153:28–46, 2001.

[7] B. A. Dubrovin. Theta functions and nonlinear equations. *Russian Math. Surveys*, 36(2):11–80, 1981.

[8] B. A. Dubrovin, R. Flickinger, and H. Segur. Three-phase solutions of the Kadomtsev-Petviashvili equation. *Stud. Appl. Math.*, 99(2):137–203, 1997.

[9] D. Gilbarg and N. S. Trudinger. *Elliptic partial differential equations of second order*. Springer-Verlag, Berlin, 2001.

[10] M Heil. *Numerical Tools for the study of finite gap solutions of integrable systems*. PhD thesis, Technischen Universität Berlin, 1995.

[11] J.-I. Igusa. *Theta Functions*. Springer-Verlag, New York, 1972.

[12] C. G. J Jacobi. Fundamenta Nova Theoriae Functionum Ellipticarum. *Königsberg*, 1829.

[13] A. K. Lenstra, H. W. Lenstra, Jr., and L. Lovász. Factoring polynomials with rational coefficients. *Math. Ann*, 261:515–534, 1982.

[14] David Mumford. *Tata lectures on theta. I.* Birkhäuser Boston Inc., Boston, MA, 1983.

[15] David Mumford. *Tata lectures on theta. II.* Birkhäuser Boston Inc., Boston, MA, 1984.

[16] David Mumford. *Tata lectures on theta. III.* Birkhäuser Boston Inc., Boston, MA, 1991.

[17] G. F. B. Riemann. Theorie der Abel'schen functionen. *Journal für reine und angewandte Mathematik*, 54:101–155, 1857.

[18] C. L. Siegel. *Topics in complex function theory. Vol. III.* John Wiley & Sons, Inc., New York, 1989.

[19] B. Vallée. A central problem in the algorithmic geometry of numbers: lattice reduction. *CWI Quarterly*, 3:95–120, 1990.

[20] E. T. Whittaker and G. N. Watson. *A course of modern analysis*. Cambridge University Press, Cambridge, 1902.

[21] W. Wirtinger. *Untersuchungen über thetafunctionen*. B. G. Teubner, Leipzig, 1895.

Alexander Bobenko, Matthias Heil, Markus Schmies
Fachbereich Mathematik
Technische Universität Berlin
Strass des 17.Juni 136
10623 Berlin, Germany
bobenkosfb288.math.tu-berlin.de
mattheil-lanzinger.de
schmiessfb288.math.tu-berlin.de

Bernard Deconinck
Department of Mathematics
Colorado State University
Fort Collins, CO 80524-1874, USA
deconincmath.colostate.edu

Mark van Hoeij
Department of Mathematics
Florida State University
Tallahassee, FL 32306, USA
hoeijmath.fsu.edu